Cold-formed Steel-Concrete Composite Beams with Back-to-Back Channel Sections in Bendin

Rajić, Andrea; Lukačević, Ivan; Skejić, Davor; Ungureanu, Viorel

Cold-formed Steel-Concrete Composite Beams with Back-to-Back Channel Sections in Bending

Article *in* Civil Engineering Journal · October 2023

DOI: 10.28991/CEJ-2023-09-10-01

4 authors:

Andrea Rajić
University of Zagreb
19 PUBLICATIONS **51** CITATIONS
SEE PROFILE

Ivan Lukačević
University of Zagreb Faculty of Civil Engineering
93 PUBLICATIONS **226** CITATIONS
SEE PROFILE

Davor Skejic
University of Zagreb Faculty of Civil Engineering
96 PUBLICATIONS **316** CITATIONS
SEE PROFILE

Viorel Ungureanu
Polytechnic University of Timisoara
158 PUBLICATIONS **1,378** CITATIONS
SEE PROFILE

Available online at www.CivileJournal.org

Civil Engineering Journal

(E-ISSN: 2476-3055; ISSN: 2676-6957)

Vol. 9, No. 10, October, 2023

Cold-formed Steel-Concrete Composite Beams with Back-to-Back Channel Sections in Bending

Andrea Rajić [1], Ivan Lukačević [1*], Davor Skejić [1], Viorel Ungureanu [2, 3]

[1] *Faculty of Civil Engineering, University of Zagreb, 10000 Zagreb, Kačićeva 26, Croatia.*

[2] *Department of Steel Structures and Structural Mechanics, Politehnica University of Timisoara, 300224 Timisoara, Ioan Curea 1, Romania.*

[3] *Laboratory of Steel Structures, Romanian Academy, Timisoara Branch, 300223 Timisoara, Mihai Viteazu 24, Romania.*

Received 23 May 2023; Revised 07 September 2023; Accepted 20 September 2023; Published 01 October 2023

Abstract

Steel-concrete composite structures are very attractive because of their characteristics, which can be emphasised by using cold-formed steel instead of hot-rolled ones. This paper presents possible analytical approaches and a parametric finite element study of cold-formed steel-concrete composite beams in bending. Analysed beams are formed of back-to-back cold-formed steel channels and concrete slabs connected by demountable shear connectors. A solid concrete slab on a profiled metal sheet analysed. Also, the study investigates the influence of corrugated web between the back-to-back channels of different thicknesses. In the case of a corrugated web, the distance between the shear connectors is increased. Furthermore, different degrees of shear connection, shear connector quality, and their arrangements are considered. An analytical study is based on full and partial shear connection assumptions and non-linear bending resistance. It is shown that the steel channel thickness and degree of shear connection significantly influence the beam bending capacity as well as concrete slab configurations. Conversely, a discrete connection between steel elements has a minor effect. A comparison of the maximum obtained bending capacities in FE analyses is in good agreement with analytical approaches for full and partial shear connections.

Keywords: Cold-Formed Steel; Steel-Concrete Composite Beams; Demountable Shear Connections; Discrete and Continuous Shear Connections; Bending Resistance; Numerical Study.

1. Introduction

In recent years, cold-formed steel (CFS) sections have become popular compared to hot-rolled sections because of their benefits, such as lower price, reduced self-weight, easier on-site handling, and faster construction. Highly efficient structural forms can be composed when using built-up CFS sections in structures. Furthermore, a higher resistance of built-up sections can be achieved by using different connection types between its components. For example, the study on the bending resistance of back-to-back built-up CFS members showed that the bending resistance of steel sections depends on the type of connection [1].

Selvaraj & Madhavan [2] investigate the current design expressions of back-to-back CFS beams by numerical study. The steel beam comprises two identical sigma sections with a thickness of 1.25 mm and is connected by spot welding. The experimental results showed that the intermediate connection spacing had a negligible influence on the ultimate capacity and failure modes. The bending capacity of a similar system, back-to-back CFS channels with edge-stiffened holes, un-stiffened holes, and plain webs, was investigated by Chen et al. [3]. Because of the lack of available literature,

* Corresponding author: ivan.lukacevic@grad.unizg.hr

http://dx.doi.org/10.28991/CEJ-2023-09-10-01

authors investigate the already-mentioned system under four-point loading. Besides the experimental research, they carried out a non-linear finite element (FE) analysis. Six specimens with edge-stiffened holes, six specimens with unstiffened holes, and two plain channels were tested. The experimental results showed that the specimens with edge-stiffened holes had an increased moment capacity by 15.4% compared to those without holes. Specimens with unstiffened holes reduced moment capacity by 15.1% compared to those without holes. Good concordance is observed between the numerical and experimental results.

Considering the importance of the connection type between CFS elements, studies [4–7] present studies about spot weld resistance and its efficiency in the system formed of CFS elements, channel sections, shear plates, and corrugated web (CW). Spot welds can provide a reliable solution for discrete connections between CFS elements.

Koudier et al. [8] present a numerical investigation of CFS members with different web shapes. Three different web shapes are investigated, and it is concluded that web corrugation increases the bending capacity and the beam stiffness, especially trapezoidal web shapes. Alharthi et al. [9] investigate the hybrid steel beams with trapezoidal CW by numerical analysis. The results show that increasing web thickness by 1 mm can change the failure mode from web buckling with flange buckling to only flange buckling. Furthermore, increased web height resulted in decreased compressive stress on the top of the flange, which could delay or prevent flange buckling. For the flanges, increased flange thickness changes the failure mode from web buckling with flange buckling to web buckling only. Also, the number of stiffeners or increased stiffener height greatly influenced the load capacity and failure mode of the steel beams with the CW. Other applications of different web shapes in CFS members are analysed in the literature [10–12]. In addition to the different web shapes used in the steel section, Fang et al. [13] investigate the web-crippling resistance of CFS channels with web holes. It is shown that American standards and Australian/New Zealand standards could closely predict the reduced web crippling strength of CFS sections under interior one-flange conditions. Thanks to the mentioned papers, it is possible to influence the beam capacity by the CW shape.

In addition to the mentioned ways of increasing the bending resistance of CFS elements, composite CFS-concrete systems have become more popular. By combining a built-up steel beam with a concrete slab, the optimal utilisation of two materials, i.e., steel and concrete, can be achieved.

The most common shear connection in composite beams with hot-rolled steel sections are headed studs. Due to their significant benefits, CFS members can provide a competitive alternative to hot-rolled steel sections by designing new built-up systems and using connecting techniques. However, different alternative solutions can be found in the literature instead of welded-headed studs in the case of CFS elements.

Hsu et al. [14] investigate new composite beams formed of reinforced concrete slabs on a profiled metal sheet with CFS joists and continuous shear connectors. It is concluded that the continuous, cold-formed furring shear connector could help distribute the horizontal shear force. Furthermore, it is shown that composite sections behave similarly to non-composite sections after the longitudinal shear crack in the concrete slab appears. In addition, it was noticed that the composite and non-composite specimens had similar load-deflection behaviour at the initial stage. Compression buckling was noticed in non-composite specimens when the concrete slab started to crack in the final stage. This is the consequence of the help of a continuous shear connector that moved the neutral axis upwards to the concrete slab.

Bamaga et al. [15] investigate the structural behaviour of lipped CFS channel sections combined with concrete slabs in composite beams. The laboratory tests were conducted on two no-composite and six composite specimens. Three types of shear connectors were used: single-bracket shear connector, double-bracket shear connector and hot-rolled plate shear connector. The observed parameters were the type of shear connector and the thickness of the CFS section (2.0 mm and 2.3 mm). As expected, the main conclusion is that a composite beam has higher moment capacities and stiffness than a non-composite beam. Furthermore, considering the ultimate load, the composite beam failed due to the combination of maximum bending and shear force. In addition, comparing the experimental results and analytical values using the plastic theory, the values were similar. Double-bracket shear connectors showed an increased maximum moment capacity compared to the other shear connectors. A numerical study for this research is presented in Elsawaf & Bamaga [16], in which the strength capacity and failure mode of shear connectors suitable for cold-formed composite steel beams are investigated. In addition to previously studied shear connectors, the headed studs were also investigated. The headed stud shear connector was 76 mm high and welded to the steel beam flange. The research concludes that the concrete damaged plasticity model can allow a concrete slab crushing and longitudinal crack, which is a common failure for all specimens. Furthermore, in the case of a double-bracket shear connector, the proposed FE models clearly capture the slip between the concrete slab and the metal sheet. In the case of the headed stud shear connector, the FE models have captured the failure modes of headed stud shear connector specimens. At the same time, no cracks were observed on the concrete slab.

In recent years, a demountable connection between steel and concrete elements has been one of the most popular types of connection. Demountability is commonly achieved with different types of demountable bolts [17]. Knowing that the reuse of steel elements should be increased to reduce footprint impact, Nijgh et al. [18] investigates the elastic

behaviour of a tapered steel-concrete composite beam optimised for reuse. It emphasises the direction of the market for the reuse of steel components. A full and partial shear connection can be obtained when the shear connectors are placed in different arrangements. The partial shear connection can be achieved by placing the bolts in a continuous arrangement with bolts in pairs or a staggered arrangement of bolts. With a staggered arrangement and a controlled degree of shear connection, it is possible to reduce the number of bolts and, simultaneously, the cost and construction time. A composite system with demountable bolts and the precast ferro-cement slab was investigated in [19, 20]. This study used nine simply supported beam specimens composed of back-to-back lipped C-sections connected with self-drilling screws and ferro-cement slabs connected by structural bolts as shear connectors. Based on the experimental results and observations, specimens with a CFS section of 3 mm and 4 mm thickness failed due to ferro-cement crushing. Specimens with CFS sections of 2 mm thickness failed due to buckling of the steel section. The shear connectors provided a full shear connection, transferring the longitudinal shear force from the slab to the steel without failure. Furthermore, demountable shear connectors were analysed in the paper by Hosseini et al. [21]. Their article is a research on using blind bolts as an innovative solution to achieve a demountable shear connection. The results showed that the shear capacity of the bolted shear connectors was improved by increasing the height of the blind bolt shear connector. Also, the load-bearing capacity of blind bolted connections was affected by increasing the friction coefficient of the contact surfaces between the blind bolts and the steel-concrete interfaces. In addition to the mentioned investigations, papers [22,23] also investigate demountable shear connections.

Many investigations still deal with different types of shear connections [22–25]. FE modelling of shear connection is shown in Talukder et al. [26], Alwash & Abd [27] and Chung & Sotelino [28]. Several experimental research with different types of shear connectors are explained in Studies [29-32]. Elsawaf & Bamaga [16] investigate the failure modes of shear connectors suitable for composite cold-formed steel beams, while design rules for shear connection are shown in Studies [33–35].

This paper deals with a parametric FE study and possible solutions for analytical calculations of CFS-concrete composite beams in bending. Analysed beams were formed of back-to-back CFS channels connected with discrete and continuous connections and concrete slabs by demountable shear connectors. Two configurations of concrete slabs were analysed: solid or slab on a profiled metal sheet. Furthermore, the study investigates the influence of CW presence between back-to-back channels as well as channel thickness. The case with a CW ensures space between channels and wider space between shear connectors. Also, the research considers the influence of bolt quality on the demountable shear connection and their different arrangements. Continuous arrangements with bolts in pairs or staggered arrangements based on the geometry of the profiled metal sheet were analysed. The study consists of a comparison of the results of 142 FE models in Abaqus software. FE-obtained bending capacities are compared with the bending resistances calculated using different analytical approaches. Three different approaches are investigated to find the best results compared to numerical models. The brief methodology of the parametric study is presented by flowchart in Figure 1.

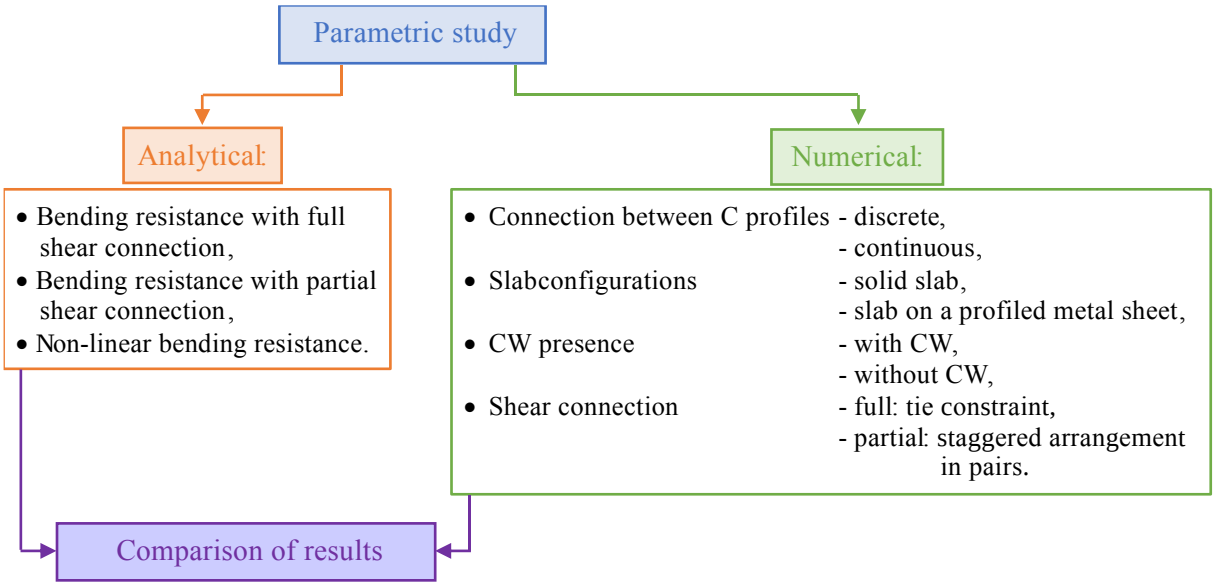

Figure 1. Flowchart of methodology

2. Analytical Assessment of Bending Resistance

The bending resistance is calculated according to three different analytical approaches. Since CFS profiles are usually classified as classes 3 or 4, their plastic resistance is impossible to achieve. The plastic resistance in a composite

section is possible if the whole steel section is in tension, which depends on the position of the plastic neutral axis. Considering this assumption and the full shear connection, the calculation of the bending moment resistance of the analysed composite section is possible, and it is presented in Section 2.1.

In the case of partial shear connection, the bending resistance is calculated using a modified Eurocode 4 approach according to Lukačević et al. [17], where the elastic bending resistance of the structural steel section replaces the plastic bending resistance of the structural steel section. The procedure is presented in Section 2.2.

Finally, non-linear bending resistance is calculated according to EN 1994-1-1 [36], Kyvelou et al. [37] and Dujmović et al. [38], and the procedure with results is shown in Section 2.3.

2.1. Approach 1: Bending Resistance with Full Shear Connection

To provide an analytical resistance of the CFS-concrete cross-section, the first and the most crucial parameter is the position of the neutral axis, which must be checked. For all models with full shear connection, the position of the neutral axis, $x_{pl,k}$, for the characteristic value of the concrete compressive strength can be calculated by Equation 1.

$$x_{pl,k} = \frac{2 \cdot A \cdot f_{yk}}{b_{eff} \cdot 0.85 \cdot f_{ck}} \quad (1)$$

where A is the cross-section area of the CFS channel section (presented in Table 1), f_{yk} is the characteristic yield strength of steel, b_{eff} is the total effective width, f_{ck} is the characteristic value of concrete compressive strength.

Knowing the value of $x_{pl,k}$, it is possible to calculate the plastic bending resistance of the beam for the composite beams with metal sheets, $M_{pl,Rk}$ (Equation 2).

$$M_{pl,Rk} = 2 \cdot A \cdot f_{yk} \cdot \left(\frac{h}{2} + h_p + h_c - \frac{x_{pl,k}}{2}\right) \quad (2)$$

where h is the height of the CFS C200 channel section, h_c is the height of the concrete slab (60 mm), and h_p is the height of the profiled metal sheet rib (60 mm), see Figure 2. In the case of composite beams with solid slabs, the h_p value is zero, and the height of the concrete slab is 90 mm. The calculated values of the plastic bending resistances for the full shear connection are shown in Table 1.

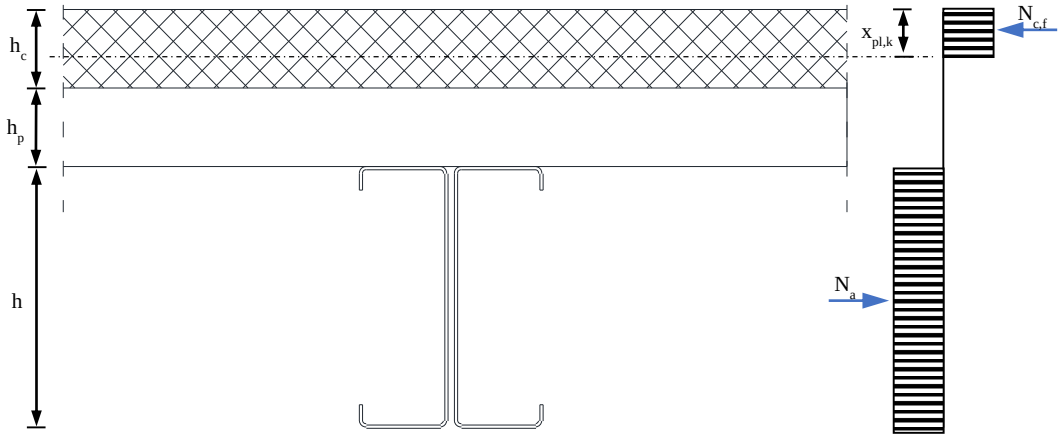

Figure 2. Cross section of the beam with concrete slab on profiled metal sheet

Table 1. Calculation of plastic bending resistance characteristic values - approach 1

Thickness of C200 channel section [mm]	PROFILE	A [mm^2]	$x_{pl,k}$ [mm]	$M_{pl,Rk}$ [kNm]	
				h_c=90 mm	h_c+h_p=120 mm
2.0	C200/2.0	717	15.7	91.4	106.5
2.5	C200/2.5	895	19.7	112.9	131.7
3.0	C200/3.0	1089	23.9	135.7	158.6

2.2. Approach 2: Bending Resistance with Partial Shear Connection

For the calculation of the shear connection degree, it is necessary to know the arrangement of shear connectors and the values of forces in the steel cross-section (3), N_a, and the concrete slab (4), N_c. According to the calculated position of the neutral axis shown in Table 1, the neutral axis is in the concrete slab.

$$N_a = 2 \cdot A \cdot f_{yk} \quad (3)$$

$$N_c = x_{pl,k} \cdot b_{eff} \cdot 0.85 \cdot f_{ck} \quad (4)$$

$$F_l = N_a = N_c \quad (5)$$

Equation 6 gives the required number of shear connectors for a full shear connection, n_{full}.

$$n_{full} = \frac{F_l}{n \cdot P_{Rk,min}} \quad (6)$$

where F_l is a longitudinal force in composite action, n is the number of shear connectors in the cross-section and $P_{Rk,min}$ is a minimum value between two calculated for the characteristic shear resistance of the shear connectors (depending on the possible failure mode in the shear connection).

The plastic neutral axis is located in the concrete slab for beams investigated and $F_l = 2 \cdot A \cdot f_{yk}$ or $F_l = x_{pl,k} \cdot b_{eff} \cdot 0.85 \cdot f_{ck}$.

According to EN 1994-1-1 [36], the resistance of shear connectors is defined by the following equations:

$$P_{Rk} = min\{P_{Rk,1}, P_{Rk,2}\} \quad (7)$$

$$P_{Rk,1} = 0.8 \cdot f_u \cdot \pi \cdot d^2/4 \quad (8)$$

$$P_{Rk,2} = 0.29 \cdot \alpha \cdot d^2 \cdot \sqrt{f_{ck} \cdot E_{cm}} \quad (9)$$

where f_u is the specified ultimate tensile strength of the material of the shear connectors, d is the diameter of the shear connector, E_{cm} is the secant modulus of elasticity of concrete and α is a parameter that depends on the ratio of the nominal height of the shear connector and the shear connector diameter.

Even though these equations are calibrated for headed studs with a tensile strength of up to 500 MPa, they are assumed to be valid for bolts with a tensile strength of 800 MPa. Furthermore, to calculate the resistance of shear connectors, in the case of a concrete slab on a metal sheet with ribs perpendicular to the beam, it is necessary to reduce its resistance by the reduction factor kt given in EN 1994-1-1 [36].

After calculating the bolt resistance with Equations 7 to 9, it is possible to find out the degree of shear connection and the bending resistance of the considered cross sections.

For the analysed composite beams, the longitudinal distance of the bolts in the composite beams is 240 mm, which leads to nine bolts in the case of a staggered arrangement of bolts or nine bolt pairs in the case of continuous bolts arrangement in the shear span. The degree of shear connection is calculated by the following Equation 10:

$$\eta = \frac{n}{n_{full}} \quad (10)$$

where n is the number of bolts (or pair of bolts) on the shear span.

According to Lukačević et al. [17] and EN 1994-1-1 [36], knowing the degree of shear connection, it is possible to calculate the bending resistance - for the partial shear connection - by Equation 11:

$$M_{Rk} = M_{el,a,Rk} + \left(M_{pl,Rk} - M_{el,a,Rk}\right) \cdot \eta \quad (11)$$

Equation 11 is a modified equation from EN 1994-1-1 [36] where the plastic resistance of the steel section, $M_{pl,a,Rk}$, is replaced by the elastic bending resistance of the steel cross-section, $M_{el,a,Rk}$.

The results of the analytical calculations are shown in Tables 2 to 4 for the cases of solid concrete slab and when concrete slab lays on a metal sheet when bending resistance (M_{Rk}) is calculated with and without reduction factor, k_t

Table 2. Bending resistances for beams with CFS C200/2.0 – approach 2

Slab configuration	Shear connection type	Degree of shear connection		Bending resistance [kNm] (M_{Rk} with /without k_t)	
solid slab	TIE, sc12C, sc12S	1.0		91.4	
Concrete slab on a profiled metal sheet	TIE, sc12C	1.0		106.5	
	sc12S	0.9	1.0	98.5	104.5

Table 3. Bending resistances for beams with CFS C200/2.5 – approach 2

Slab configuration	Shear connection type	Degree of shear connection		Bending resistance [kNm] (M_{Rk} with /without k_t)	
Solid slab	TIE, sc12C, sc12S	1.0		112.9	
Concrete slab on a profiled metal sheet	TIE, sc12C	1.0		131.7	
	sc12S	0.7	1.0	102.1	131.7

Table 4. Bending resistances for beams with CFS C200/3.0 – approach 2

Slab configuration	Shear connection type	Degree of shear connection		Bending resistance [kNm] (M_{Rk} with /without k_t)	
Solid slab	TIE, sc12C, sc12S	1.0		135.7	
Concrete slab on a profiled metal sheet	TIE	1.0		158.6	
	sc12C	0.8	1.0	137.9	158.6
	sc12S	0.6	1.0	113.0	158.6

Two different bolt materials are investigated: bolts material with a yield strength of 640 MPa and ultimate tensile strength of 800 MPa (the designation 8.8 in the further text will be used) and material which has a yield strength of 350 MPa and ultimate tensile strength of 450 MPa (the designation 350/450 in the further text will be used) which meet the requirements given in EN 1994-1-1 [36] for the maximum ultimate tensile strength of bolts. For both analysed cases, the failure mode is concrete crushing.

2.3. Approach 3: Non-linear Bending Resistance

The third considered approach is the non-linear bending resistance. In the first step, it is necessary to calculate the elastic bending resistance of the cross-section. In the beginning, the concrete slab is reduced to a steel section. For calculating the ideal area of the composite cross-section, the ideal area of the concrete slab cross-section must be known as the distance between the centre of gravity of the composite section and the concrete slab. If the centre of gravity of the composite section is on a concrete slab, it is necessary to repeat the procedure to consider the reduced area of the concrete slab.

After calculating the part of a concrete slab in compression, the procedure must be repeated, from calculating the ideal area of the concrete slab cross-section to the distance between the centre of gravity of the composite section and the concrete slab. Knowing all the mentioned values makes it possible to calculate the moment of inertia for the concrete slab and the ideal moment of inertia for the composite section.

Finally, the stiffness of the composite cross-section can be calculated using Equation 12:

$$EI_L = E_a \cdot I_{i,L} \tag{12}$$

where E_a is the steel modulus of elasticity and $I_{i,L}$ is the ideal moment of inertia for the composite section.

Non-linear elastic resistance is considered only for propped systems. From the expressions for the maximum stresses that can be achieved in steel and concrete sections, Equations 13 and 14, it is possible to calculate the design bending moment equal to the required elastic bending resistance.

$$\vartheta_a = E_a \cdot \frac{M_{Ed,1}}{EI_L} \cdot z_a \tag{13}$$

$$\vartheta_c = E_c \cdot \frac{M_{Ed,2}}{EI_L} \cdot z_c \tag{14}$$

where E_c is the concrete modulus of elasticity, z_a is the distance from the centroid of the composite section to the end of the steel part, z_c is the distance from the centroid of the composite section to the end of the concrete part.

To choose the right expression for the elastic bending resistance given by EN 1994-1-1 [36], the value of the normal compressive force on the concrete slab that corresponds to $M_{el,Rk}$ must be known:

$$N_{c,el} = k \cdot \frac{M_{el,Rk}}{I_{i,L}} \cdot \left(A_{c,L} \cdot z_{ic,L}\right) \tag{15}$$

$$z_{ic,L} = \frac{A_a \cdot a_a}{A_{i,L}} \tag{16}$$

where k is obtained from the condition that the edge fibres of the cross-section have reached the limit stresses, $A_{c,L}$ is the ideal cross-sectional area of the concrete flange, $z_{ic,L}$ is the distance from the centre of the composite cross-section to the lower edge, a_a is the distance between the centroidal axis of the steel section and the elastic neutral axis and $A_{i,L}$ is the ideal area of the composite section.

Following conditions given in EN-1994-1-1 [36], the characteristic value of the bending resistance of a composite section is given by expressions 17 and 18:

$$N_c \le N_{c,el} \rightarrow M_{Rk} = M_{a,Rk} + \left(M_{el,Rk} - M_{a,Rk}\right) \cdot \frac{N_c}{N_{c,el}} \quad (17)$$

$$N_{c,el} \le N_c \le N_{c,f} \rightarrow M_{Rk} = M_{el,Rk} + \left(M_{pl,Rk} - M_{el,Rk}\right) \cdot \frac{N_c - N_{c,el}}{N_{c,f} - N_{c,el}} \quad (18)$$

The calculated values are shown in Figure 3. Figure 3 shows that the system with a solid slab (for bolts positioned in pairs or in a staggered arrangement) has higher bending resistance than the system with a concrete slab on metal sheets. This is the consequence of the reduction in the shear connectors resistance with k_t.

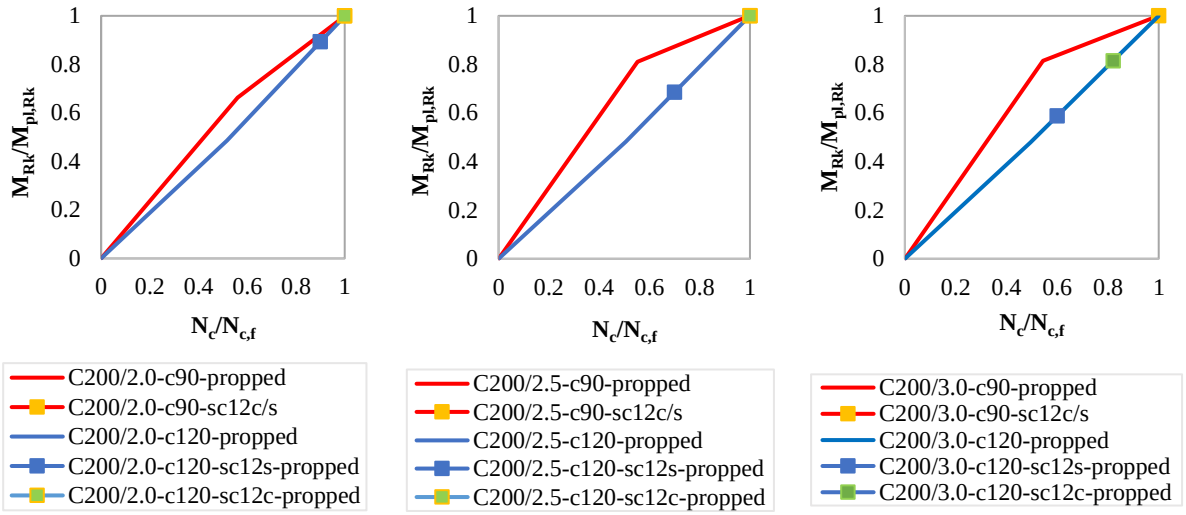

(a) thickness of channel section 2.0 mm (b) thickness of channel section 2.5 mm (c) thickness of channel section 3.0 mm

Figure 3. Simplified relationship between M and N_c

In Figure 3, a simplified relationship between M and N_c is shown. In diagrams, red curves present composite beams with a solid slab (full shear connection) and blue curves present composite beams with a metal sheet (full shear connection), both for the propped system. All diagrams are defined according to EN 1994-1-1 [36]. Analysed composite beams are calculated for the full degree of shear connection and for the cases when shear connectors are arranged in staggered arrangement and in pairs. Yellow rectangular marker marks the mentioned relationship for composite beams with a solid slab in the case when shear connectors are used. Because of no reduction by the coefficient k_t, the full shear connection is achieved for both analysed cases. This is the situation for all three diagrams that differ in the channel thickness (2.0 mm, 2.5 mm, and 3.0 mm). The calculated characteristic bending resistances according to the non-linear approach for the channel thickness of 2.0 mm with bolts in pairs and staggered arrangement are 91.4 kNm. The channel thickness of 2.5 mm with bolts in pairs and staggered arrangement resulted in characteristic resistances of 112.9 kNm. The channel thickness of 3.0 mm and bolts in pairs and staggered arrangement resulted in a characteristic resistance of 135.7 kNm. Blue and green rectangular marks show the mentioned relationship for composite beams with metal sheets in the case when shear connectors are used in pairs or a staggered arrangement, respectively. For the staggered arrangement of bolts, the values of non-linear resistances are 95.14, 90.26 and 93.08 kNm, respectively. Arrangement in pairs resulted in characteristic resistances of 106.47, 131.7, and 129.12 kNm, respectively.

3. Parametric Numerical Simulations

3.1. General

The parametric study is conducted with ABAQUS/CAE software [39]. The composite system is a 6-meter-long simply supported beam under four-point loading (six-point bending). The support conditions are defined at the reference points at the ends of the beam and are connected to the edges of the steel sections. The load is applied as a displacement in the middle of the span, and undeformable elements and coupling constraints were used for load transfer. As shown in Figure 4, the load input points are placed at a distance of 750 mm from the ends and 1500 mm from each other.

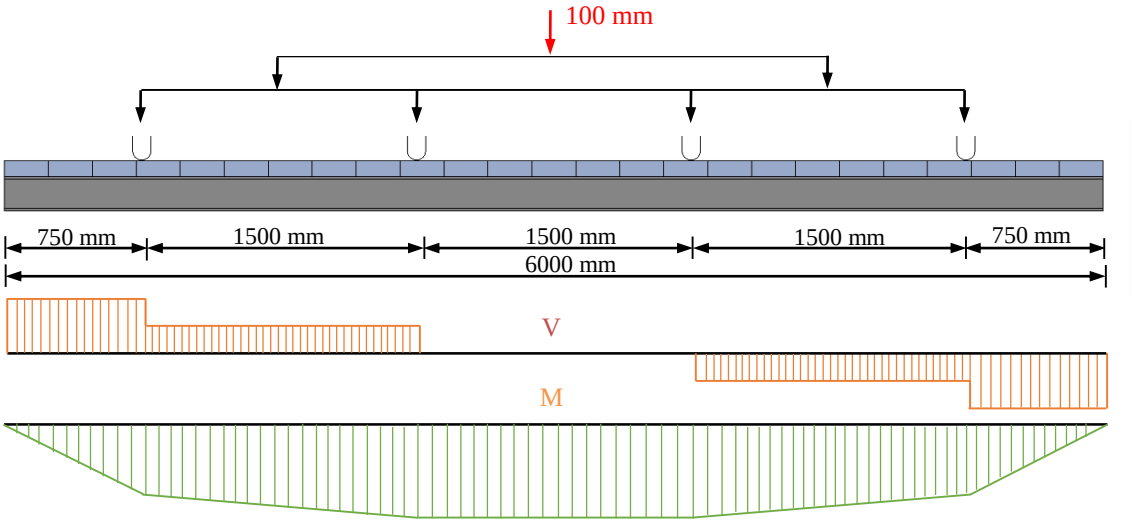

Figure 4. Static system and distribution of V and M of analysed composite beam

An explicit solver is used due to the nonlinearities of material, geometric and especially contact of the model. A time scale is used to speed up the analysis time. Dynamic impacts are avoided by keeping kinetic energy below 5% of the internal energy. Also, the limit of 1% of the wave velocity is considered in the concrete and steel parts of the model.

3.2. Geometry of Steel Beams and Concrete Slabs

As was the case in the analytical study, three different thicknesses of channel sections are analysed – 2.0 mm, 2.5 mm and 3.0 mm. The height of the channels is 200 mm, the width of the flanges is 69 mm, and the inner radius is 3 mm. The lip length depends on the thickness of the channel section. For the thickness of 2.0 mm and 2.5 mm, the lip length is 18 mm, and for the thickness of 3.0 mm is 21 mm. Furthermore, two different configurations of steel beams are considered. The first beam configuration comprises two back-to-back CFS channel sections Figure 5-a, and the second comprises two CFS channel sections with the CW, which ensures the distance between the channel sections, Figure 5-b. The CW located between the channel section has a thickness of 1 mm and extends along the entire beam length. The width of the CW rib is 60 mm, as shown in Figure 5-b.

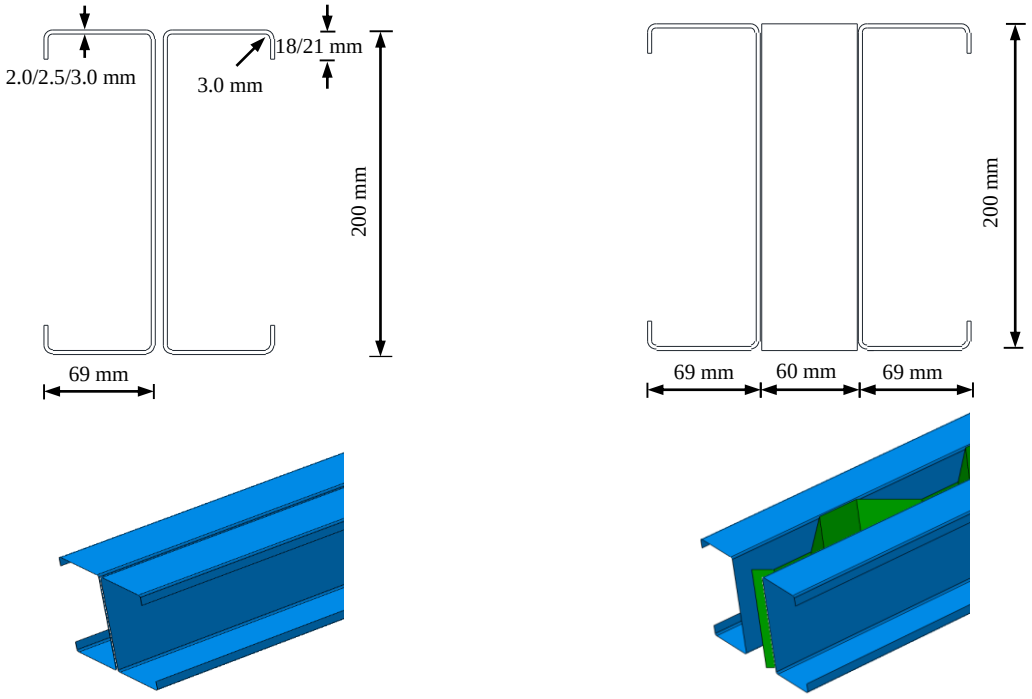

(a) Two back-to-back channel C200 sections (b) Two back-to-back channel C200 sections with CW

Figure 5. Analysed steel beam configurations

As considered in the analytical assessment, a solid slab with a height of 90 mm and a concrete slab on a profiled metal sheet whose ribs are transverse to the beam with an overall height of 120 mm were analysed. Investigated concrete

slabs are combined with steel beams presented in Figure 5. Those combinations resulted in four different composite beam configurations, in further text model 1, model 2, model 3, and model 4, presented in Figure 6.

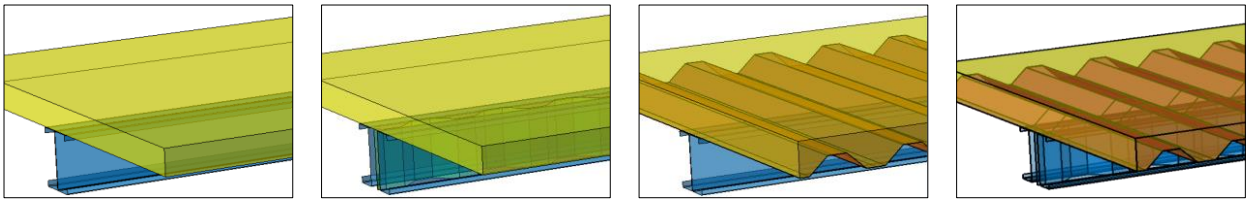

(a) Model 1 (b) Model 2 (c) Model 3 (d) Model 4

Figure 6. Analysed composite beam configurations

3.3. Material, Mesh, Finite Element Types and Contacts

The numerical models are formed by combining the shell and solid finite elements. The steel elements are defined as a 3D shell element S4R, while the concrete slab has an assigned element type C3D8R [40]. The concrete class used in the analyses is C25/30. The modulus of elasticity, E_{cm}, for C25/30 is considered 31476 MPa and the Poisson's ratio for concrete elements is 0.2, according to Lukačević [17] and EN 1992-1-1 [41]. The concrete slab has an effective width of 1500 mm. Three different mesh sizes of the concrete slab were investigated: 15 mm, 30 mm and 60 mm. Bending capacity for approximate mesh sizes of 15 and 30 mm is close for most of the analysed models.

Consequently, the adopted mesh size used for a concrete slab of the analysed system in a parametric study is 30 mm, which also significantly reduces analysis time-cost compared to the mesh size of 15 mm. Concrete damage plasticity model (CDP) is used to model concrete slab. It is based on two failure mechanisms of tensile cracking and compressive crushing of concrete [41, 42]. Furthermore, ways of modelling steel and concrete materials are presented in the paper Lukačević et al. [17]. The stress-strain relation for the used concrete C25/30 is shown in Figure 7, according to Lukačević et al. [17].

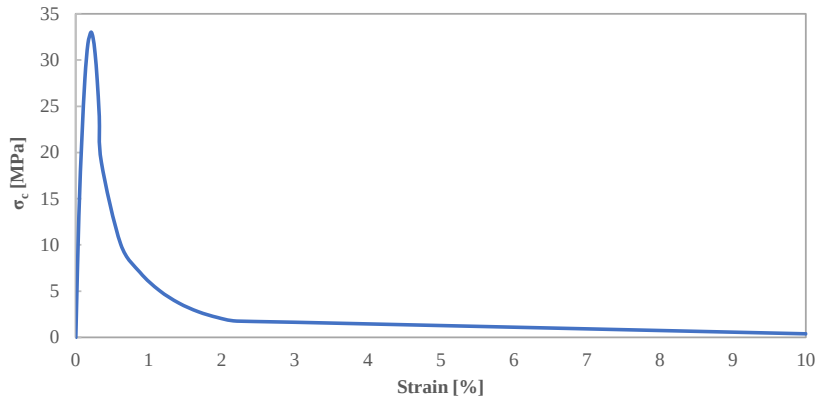

Figure 7. Stress-strain relation for C25/30

The CFS channels are modelled with S4R shell finite elements. The material characteristics of steel are defined with the bilinear elastic-plastic model. Used steel grade S350GD is defined with a nominal yield strength of 350 MPa and ultimate tensile strength of 420 MPa, which is reached at a strain of 15% [43], as shown in Figure 8. The approximate global mesh size for steel elements is 20 mm [40].

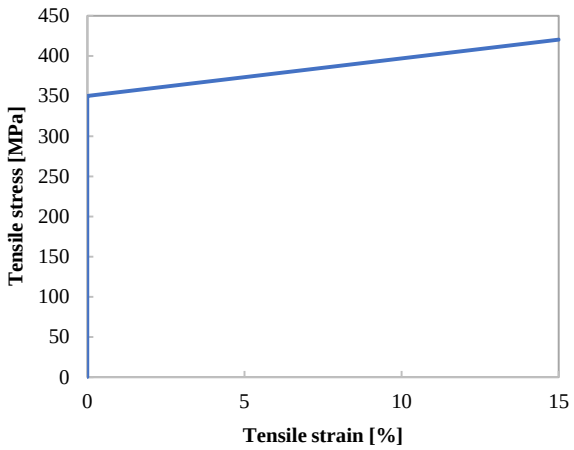

Figure 8. Nominal tensile stress-strain relation for steel grade S350GD

Two materials were used for bolts. A material with a yield strength of 640 MPa and ultimate tensile strength of 800 MPa (the designation 8.8 in the further text will be used) and material which has a yield strength of 350 MPa and ultimate tensile strength of 450 MPa (the designation 350/450 in the further text will be used). The strain for the ultimate tensile strength is 12 % [43]. The modulus of elasticity of all steel elements is taken as 210 GPa, and the density of all steel elements is assumed to be 7850 kg/m^3. General contacts between all elements in the models are used. Tangential behaviour with penalty friction formulation and friction coefficient 0.3 and normal behaviour as hard contact with allowed separation after contact is used.

3.4. Type of Shear Connection

Two types of shear connections can be achieved: full and partial shear connections. Full shear connection is achieved through the tie connection given by the Abaqus/CAE software options [39]. This type of connection prevents any slip between the chosen surfaces. In order to achieve a partial shear connection, bolts of 12 mm diameter, M12, are used. Two different bolt arrangements in the longitudinal direction are considered in pairs (continuous arrangement – Figure 9-a) and a staggered arrangement (Figure 9-b).

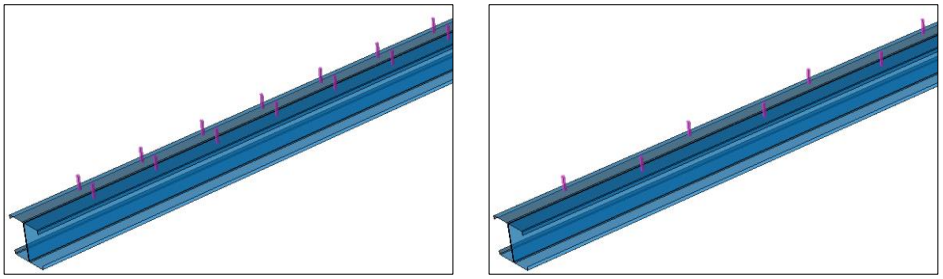

(a) Continuous arrangement of bolts (b) Staggered arrangement of bolts

Figure 9. Longitudinal bolt arrangements

The longitudinal distance between the bolts is 240 mm, which is the axial distance of the ribs of a profiled metal sheet. Furthermore, observing the analysed composite cross-section, because of two configurations of steel beams, two different transversal bolt arrangements are analysed, Figure 10. In Models 1 and 3, the distance between bolts in the composite cross section is 69 mm because the channel sections are connected back-to-back. Models 2 and 4 have a larger distance between bolts in the composite cross section (129 mm) because of inserting the CW between CFS sections.

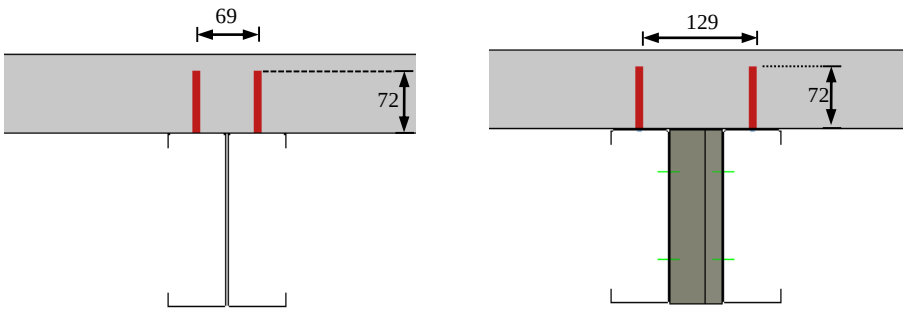

(a) Models 1 and 3 (b) Models 2 and 4

Figure 10. Transversal bolt arrangements

In Models 1 and 2, where the concrete slab is solid, the height of the bolts is considered to be 80% of the thickness of the concrete slab, which leads to the height of the bolt of 72 mm. Due to the profiled metal sheet, in Models 3 and 4, the height of the concrete slab is increased to 120 mm, and EN 1994-1-1 [36] prescribes the height of the bolts 2×d above the profiled metal sheet (d is the bolt diameter). Respecting this rule, the height of the bolts is 84 mm, Figure 11.

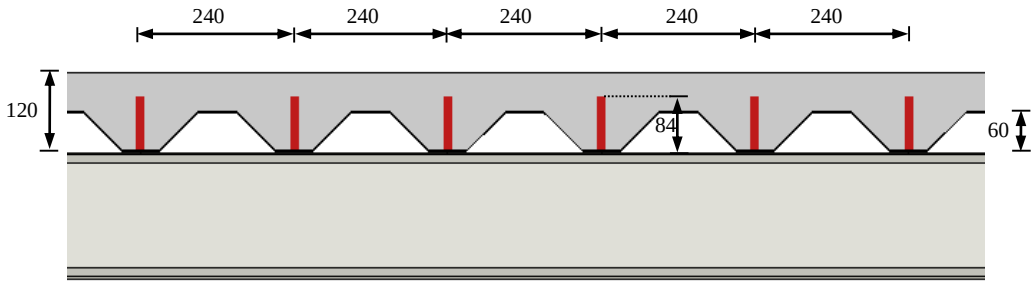

Figure 11. Height and longitudinal bolt arrangements in models 3 and 4

The bolts are embedded in the concrete slab and their bottom is connected to the top flange of the CFS C120 section by a wire element with a beam connection type. In this way, the connection between the shear connector and the channel section is ensured. As a simplification of models, bolts are defined as beam elements with a circular cross-section without a bolt head.

3.5. Type of Connection between Steel Elements

The connection between steel elements is taken into account in two different ways: by tie connection and by point-based fasteners with multi-point constraint (MPC) connector response. Such a connection can be, for example, realised by structural bolting or resistance spot welding. The vertical arrangements of the point-based fasteners are presented in Figure 12.

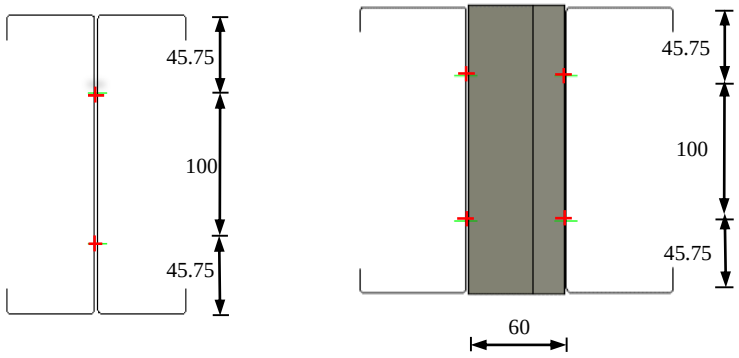

(a) in models 1 and 3 (b) in models 2 and 4

Figure 12. The vertical arrangement of the point-based fasteners

The longitudinal arrangement of point-based fasteners is presented in Figure 13. In Models 1 and 3, the distance between the end of the beam and the point-based fasteners is 240 mm. In Models 2 and 4, where the CW is between channels, the distance of the point-based fastener from the end of the beam is 50 mm, and the distance between point-based fasteners on the same channel is 240 mm. In some studies, spot welds are designed based on laboratory research that has previously been conducted [4–7]. In this study, a simplified method is used that uses the response of the MPC connector.

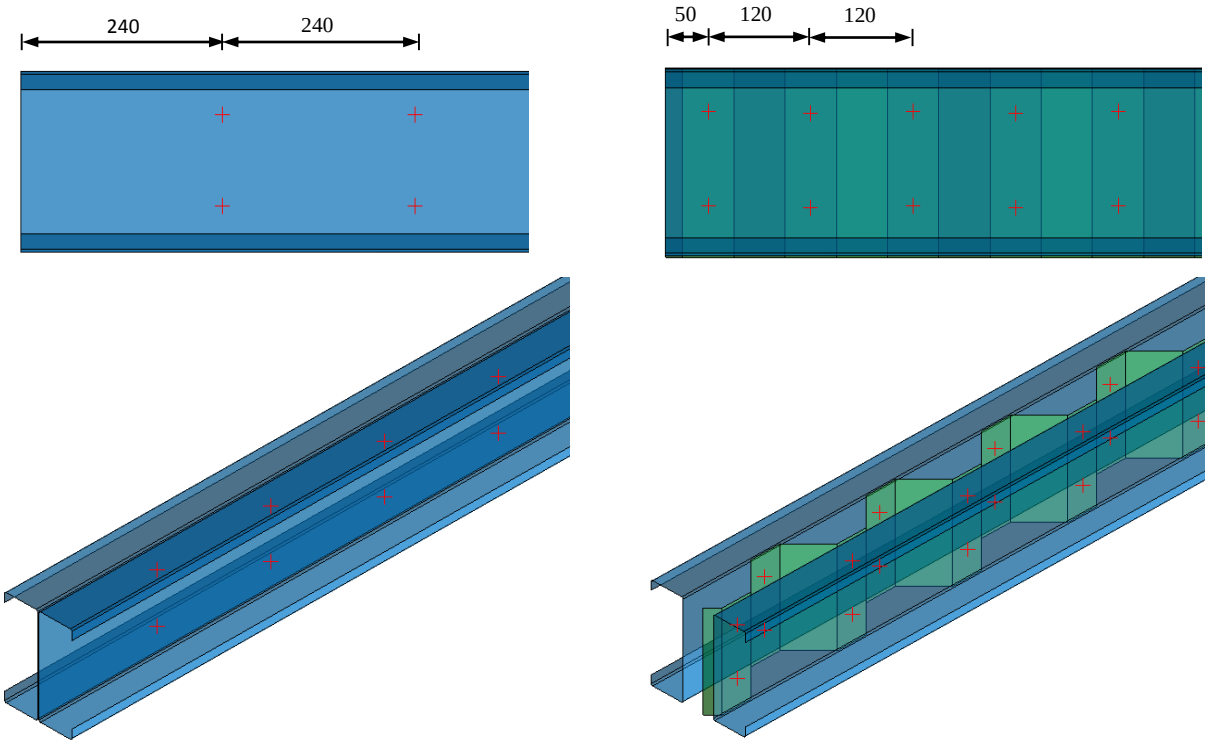

(a) in models 1 and 3 (b) in models 2 and 4

Figure 13. Longitudinal arrangement of the point-based fasteners

3.6. Nomenclature and Matrix of Analysed Models

The nomenclature of the models is shown in Figure 14. In models without CW, this part of the name disappears.

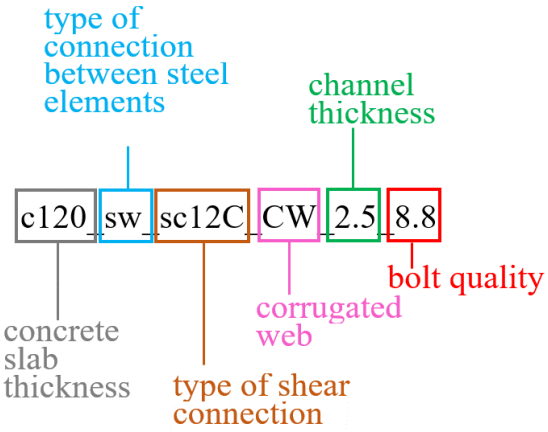

Figure 14. Nomenclature of models

Table 5 presents the matrix of analysed models. For each model, two types of bolts material and three steel thicknesses are analysed. In total, 142 models were analysed. In addition to the models presented in Table 5, 12 models without shear connection are modelled in order to show the influence of the shear connection on the bending capacity compared to models with the shear connection.

Table 5. Matrix of analysed models

Concrete slab thickness [mm]	Profiled metal sheet	Connection between steel elements	Type of shear connection	Shear connection continuous (C)/staggered (S)	CW	Channel thickness [mm]	Bolt quality
90	no	tie	tie	/	no	2.0/2.5/3.0	/
90	no	tie	sc12	C	no	2.0/2.5/3.0	8.8/ 350/450
90	no	tie	sc12	S	no	2.0/2.5/3.0	8.8/ 350/450
90	no	spot weld	tie	/	no	2.0/2.5/3.0	/
90	no	spot weld	sc12	C	no	2.0/2.5/3.0	8.8/ 350/450
90	no	spot weld	sc12	S	no	2.0/2.5/3.0	8.8/ 350/450
90	no	tie	tie	/	yes	2.0/2.5/3.0	/
90	no	tie	sc12	C	yes	2.0/2.5/3.0	8.8/ 350/450
90	no	tie	sc12	S	yes	2.0/2.5/3.0	8.8/ 350/450
90	no	spot weld	tie	/	yes	2.0/2.5/3.0	/
90	no	spot weld	sc12	C	yes	2.0/2.5/3.0	8.8/ 350/450
90	no	spot weld	sc12	S	yes	2.0/2.5/3.0	8.8/ 350/450
120	yes	tie	tie	/	no	2.0/2.5/3.0	/
120	yes	tie	sc12	C	no	2.0/2.5/3.0	8.8/ 350/450
120	yes	tie	sc12	S	no	2.0/2.5/3.0	8.8/ 350/450
120	yes	spot weld	tie	/	no	2.0/2.5/3.0	/
120	yes	spot weld	sc12	C	no	2.0/2.5/3.0	8.8/ 350/450
120	yes	spot weld	sc12	S	no	2.0/2.5/3.0	8.8/ 350/450
120	yes	tie	tie	/	yes	2.0/2.5/3.0	/
120	yes	tie	sc12	C	yes	2.0/2.5/3.0	8.8/ 350/450
120	yes	tie	sc12	S	yes	2.0/2.5/3.0	8.8/ 350/450
120	yes	spot weld	tie	/	yes	2.0/2.5/3.0	/
120	yes	spot weld	sc12	C	yes	2.0/2.5/3.0	8.8/ 350/450
120	yes	spot weld	sc12	S	yes	2.0/2.5/3.0	8.8/ 350/450

4. Results and Discussion

4.1. General

This section analyses the influence of several parameters: channel section thickness, bolt quality, degree of shear connection, spot weld density, corrugated web in the composite beam and concrete slab height. In the end, a comparison of analytical and numerical results is given. It must be noted that bolt quality, degree of shear connection and concrete slab height can be considered in the analytical calculation from all the abovementioned parameters.

4.2. Influence of Different Parameters

4.2.1. Channel Section Thickness

Figures 15-a and b show the influence of channel thicknesses from 2.0 mm to 3.0 mm with the step of 0.5 mm. It is shown that profile thickness significantly impacts bending capacity and flexural stiffness, regardless of the degree of shear connection (realised by a continuous (sc12C) or staggered arrangement (sc12S)) and the presence of CW between channels. The influence of the profile thickness is shown for the models with a different type of shear connection (sc12C/sc12S) and for different types of connections for the steel elements (tie/sw) to show that the thickness of the channel section significantly influences all analysed cases.

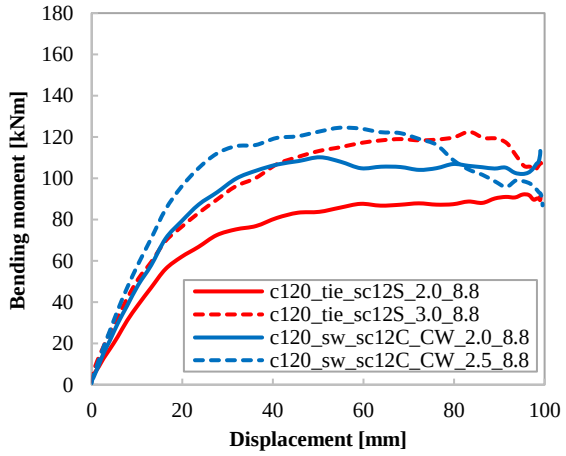

(a) models with the same bolt quality -8.8

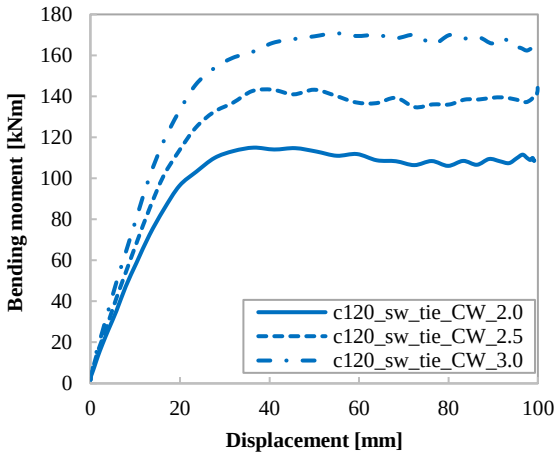

(b) models with the same degree of shear connection

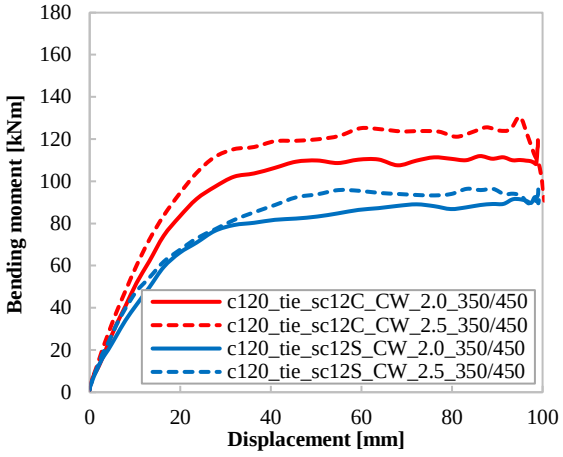

(c) models with the same bolt quality – 350/450

Figure 15. Influence of profile thickness

Figure 15-a shows the influence of the CFS channel thickness for two cases. The first case is when steel elements are connected with a tie connection (tie), and the partial shear connection is achieved by positioning the shear connectors (quality 8.8) in a staggered arrangement (sc12S). The second case is when steel elements are connected with spot welds (sw) to CW and shear connectors are placed in pairs (sc12C) in each rib of the profiled metal sheet. When the results between the same characteristics except for the channel thickness are compared, it can be concluded that increasing the channel thickness can achieve a higher bending capacity and flexural stiffness. Figure 15-b shows the influence of the channel thickness change for models with a degree of shear connection of 1.0 (tie), i.e., full shear connection and in the cases where steel elements are connected by spot welds (sw). When results for models with 2.0 mm and 2.5 mm thicknesses are compared, the bending capacity increases approximately for the same difference as in the case of 2.5 mm and 3.0 mm thicknesses. Figure 15-c shows the results for the case when the shear connectors quality is changed to 350/450 and the steel elements are connected by tie connection (tie).

Figures 16-a and 16-b show von Mises stresses in the last step frame of the analysis for the channel thicknesses of 2.0 mm and 3.0 mm. Maximum values are achieved at the lower channel flanges, and higher stress is achieved for a model with a thinner channel section, Figure 16-a.

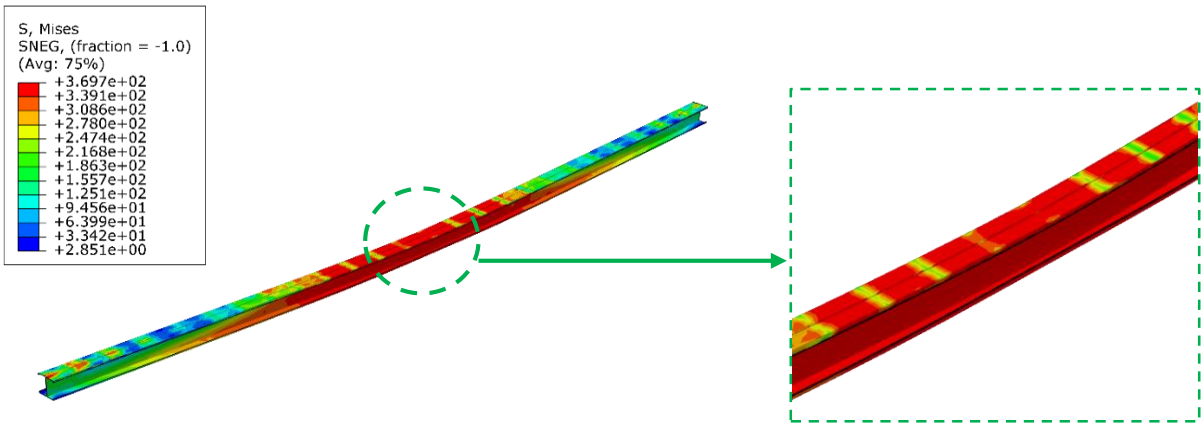

(a) c120_sw_tie_CW_2.0

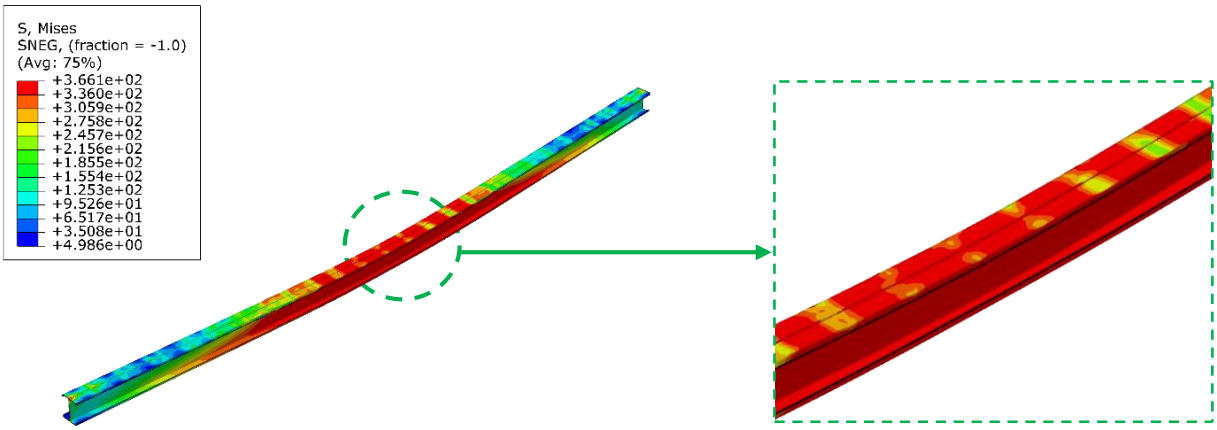

(b) c120_sw_tie_CW_3.0

Figure 16. Von Mises stress in CFS channel sections

4.2.2. Bolt Qualities

Numerical analyses show negligible differences in bending capacity and flexural stiffness when the models with shear connectors quality 8.8 are compared with shear connectors quality 350/450 (see Figures 17 a to c). This conclusion has also resulted from the analytical calculation. The reason is that the concrete crushing before the shear connectors failed.

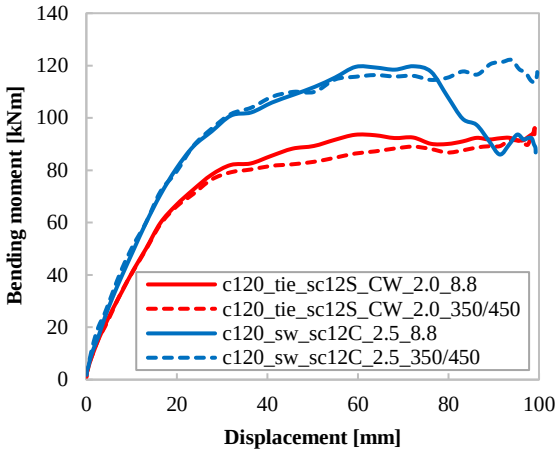

(a) models with and without CW

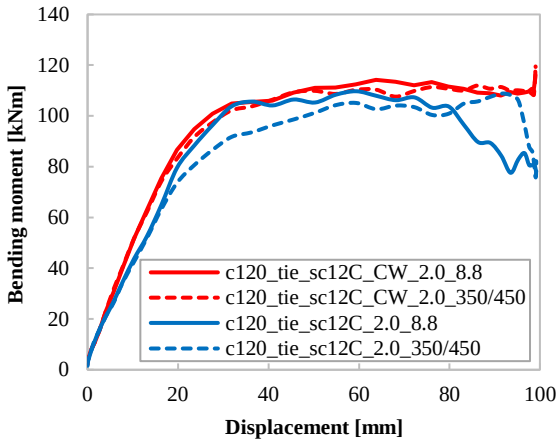

(b) models with the 2.0 mm thickness of the channel

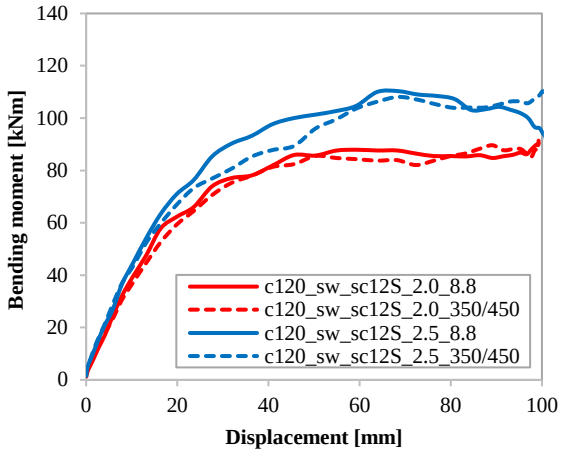

(c) models with spot-welded steel elements

Figure 17. Influence of bolts qualities

Figure 17-a shows the influence of the bolt qualities for two cases. The first case is when the steel members are tied and the CW is connected to a channel of 2.0 mm thickness. In this case, the shear connection is achieved by shear connectors positioned in a staggered arrangement (sc12S). The second case is when the channels of 2.5 mm thickness are connected by spot welds back-to-back, and shear connectors are positioned in pairs (sc12C) in each rib of the profiled metal sheet. From a comparison of the results for models with the same characteristics except for the bolt qualities, it is concluded that the bending behaviour is very similar. Figures 17-b and 17-c show the same effect for models with and without CW, different bolt quality and channel thickness.

Figures 18-a and 18-b show the inelastic deformation of the material 'PEEQ' (Equivalent Plastic Strain) for the analysed bolt qualities. The values of PEEQ in Figures 18-a and 18-b correspond to the time step when the maximum load is achieved. For a model with a bolt's quality of 8.8, the time step is 0.25; for a model with a bolts quality of 350/450, the time step is 0.2875. Considering that the PEEQ variable is higher than zero, the steel starts yielding in the step times mentioned.

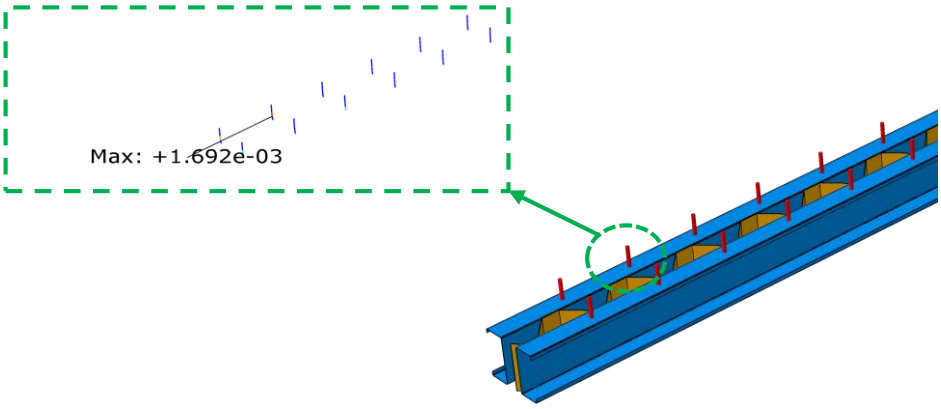

(a) bolts' quality 8.8

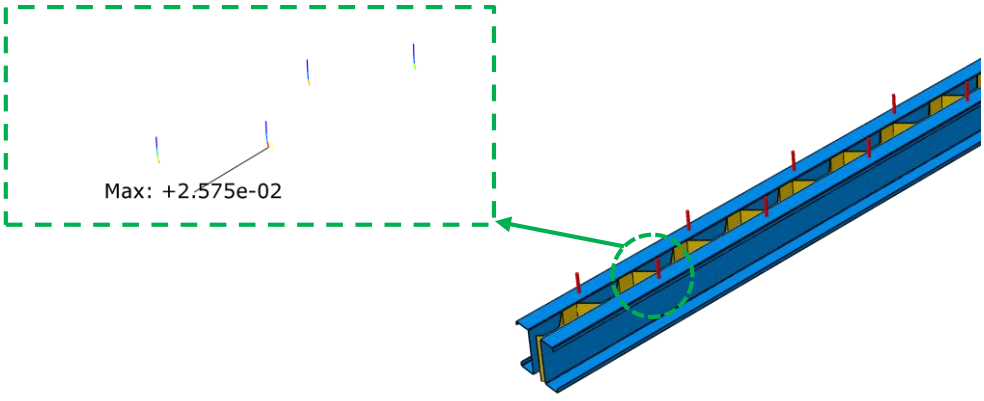

(b) bolts' quality 350/450

Figure 18. PEEQ values for model c120_tie_sc12C_CW_3.0

4.2.3. Degree of Shear Connection

The degree of shear connection is one of the most important variables that need to be considered in observing the bending capacity of the composite beam. The influence of the shear connection is presented in Figure 19. Diagrams in Figure 19 compare results for models without shear connection (sc0) and with full shear connection (tie). In results for models without shear connection (sc0), where the degree of shear connection is zero, the concrete slab lays on a built-up steel beam composed of tied CFS elements. The connection between the steel beam and the concrete slab is achieved only through general contact with friction.

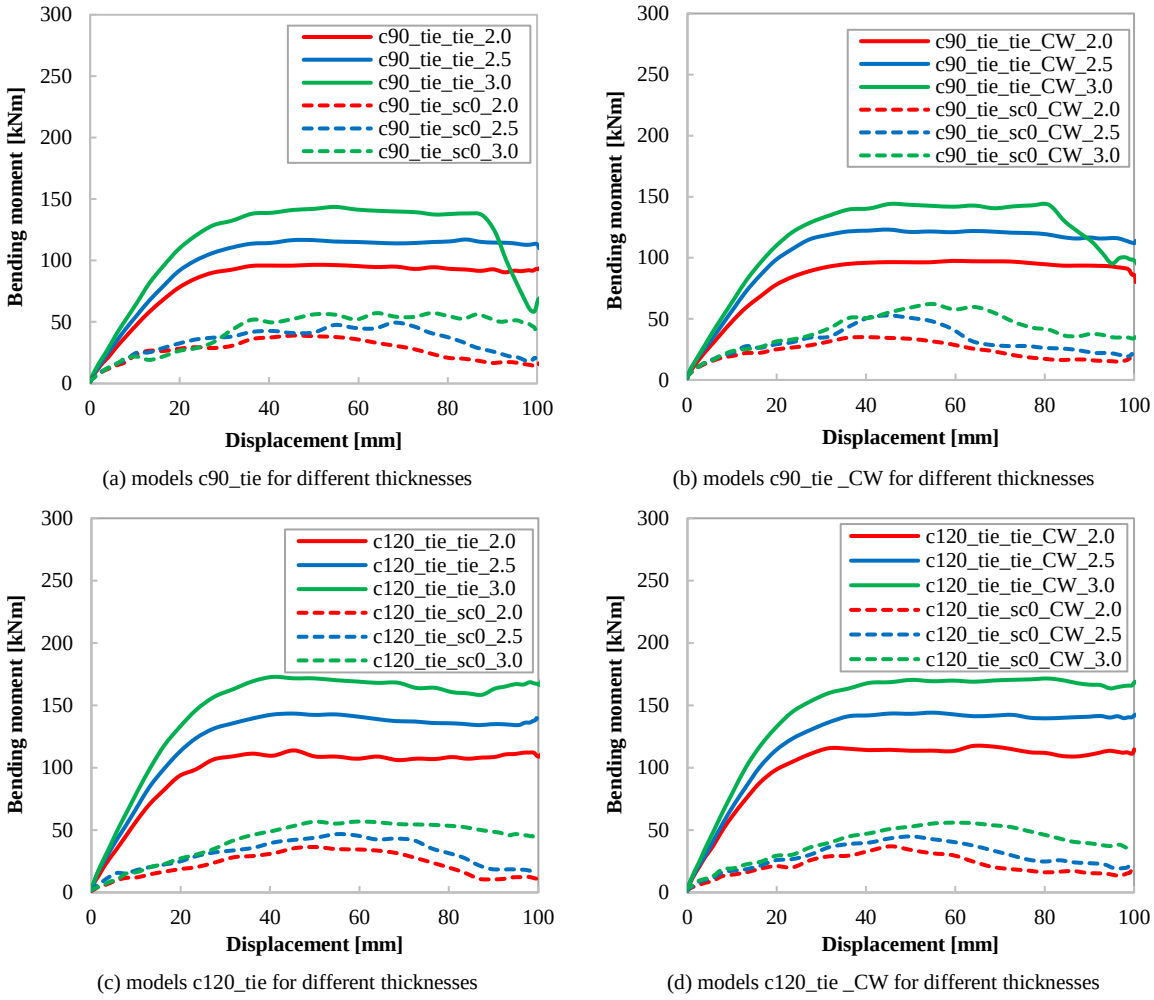

(a) models c90_tie for different thicknesses

(b) models c90_tie _CW for different thicknesses

(c) models c120_tie for different thicknesses

(d) models c120_tie _CW for different thicknesses

Figure 19. Comparison of models without shear connection and with full shear connection

These are two extreme cases of the shear connection of a composite beam. The bending capacity in the cases of full shear connection (tie) and beam flexural stiffness are significantly increased. Furthermore, the influence of the increased thickness of the CFS channel is more visible in these cases with a full shear connection. It is a consequence of composite action achieved by a tie connection between the concrete slab and the channel profiles.

By comparing results for models with and without CW with a degree of shear connection of 0 (sc0) with the same concrete slab height from Figures 19-a to 19-d, it is concluded that models without shear connection and with the same channel thickness, despite the difference in concrete slab height, achieve the same level of bending capacity and flexural stiffness. The reason for such a result is that in the system without a shear connection (sc0), only the steel beam takes the load. Also, it is concluded that bending capacities between Figures 19-a and 19-b, as well as Figures 19-c and 19-d, between models without shear connection and the same channel thickness are the same, which means that CW does not contribute to the bending capacity and flexural stiffness. Observing the results for models with full shear connection (tie), it is concluded that models with a greater height of concrete slab (c120) achieve greater bending capacity and flexural stiffness than the models with the height of the concrete slab of 90 mm (c90). Also, analysing models from Figure 19. with the same channel thickness and with and without CW, a small increase in bending capacity can be observed. Small differences can be justified due to tie connection between steel elements.

The degree of shear connection greatly impacts the results of all four analysed models (Models 1-4 from Figure 6). Figures 20-a to 20-e show how the bending capacity and flexural stiffness can significantly change depending on the

position of the shear connectors. When comparing bending capacity between models with shear connectors positioned in pairs or in a staggered arrangement, the difference in capacity is approximately 25 kNm. Figure 20-a presents results for models with tied steel elements and with different arrangements of shear connectors (sc12C and sc12S), where channel thicknesses are 2.0 and 2.5 mm. It can be observed that despite the different channel thickness, bolt quality and presence of CW, models with shear connectors positioned in pairs (sc12C) have approximately the same percentage of higher bending capacity than models with staggered bolts (sc12S). The bending capacity is approximately increased by 20%. Figure 20-b shows results for models with concrete slab height of 120 mm (c120) and channel thickness of 2.5 mm and 3.0 mm with different bolt quality and different types of connection between steel elements. For both mentioned cases, the bending capacity is increased for 25-30 kNm. Similar behaviour is observed for models with solid slabs shown in Figures 20-c to 20-e. In Figures 20-c to 20-e, models with CW and channel thickness of 3.0 mm are analysed with different bolt qualities. It is shown that the difference in bending capacities between models is similar

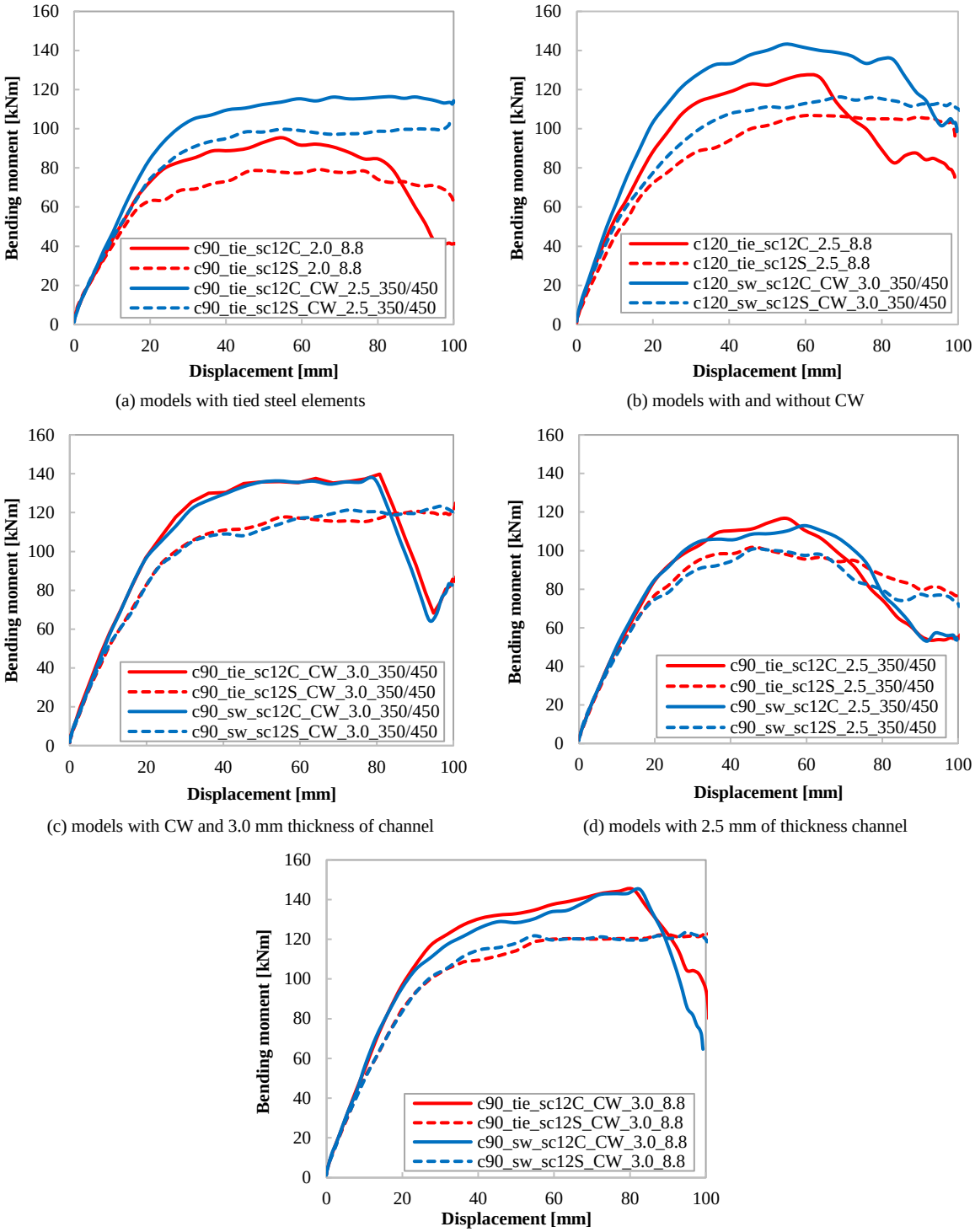

(a) models with tied steel elements

(b) models with and without CW

(c) models with CW and 3.0 mm thickness of channel

(d) models with 2.5 mm of thickness channel

(e) models with 3.0 mm of channel thickness

Figure 20. Influence of degree of shear connection

From all presented results for shear connection, it can be concluded that the degree of shear connection greatly influences the bending capacity and flexural stiffness of the analysed composite beams. Specifically, for analysed models, bending capacity can be increased by approximately 25-30% by positioning shear connectors in pairs compared to a staggered arrangement.

4.2.4. Spot Weld Density

The influence of spot weld density for different channel thicknesses is shown in Figures 21-a to 21-e. The influence of two spot welds (sw) is negligible on the models compared to those models with tied steel elements (tie). The reason for such a result is that spot weld characteristics are set to rigid MPC and the steel beam is unaffected by global stability. Results also show that it is possible to achieve the same bending capacity and flexural rigidity level by discrete connection as in models with tied steel elements.

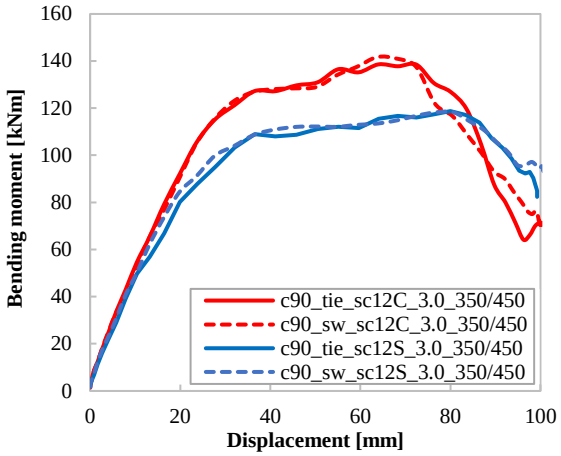

(a) model 1 with bolts 350/450

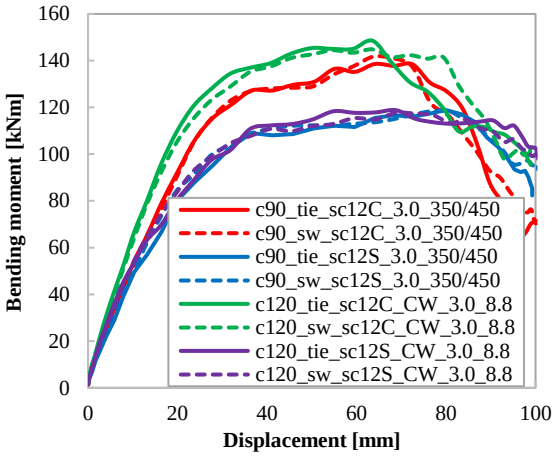

(b) models 1 and 4 with bolts 8.8 and 350/450

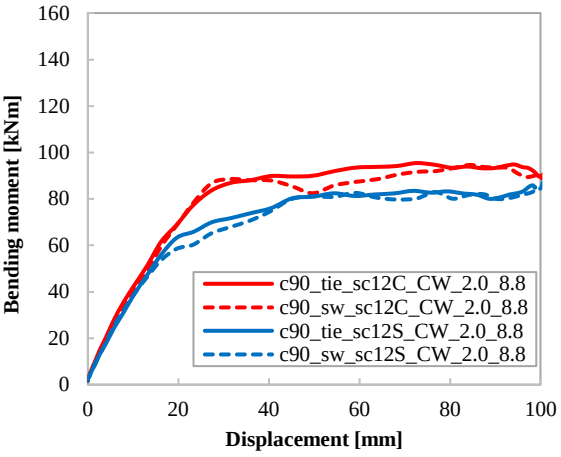

(c) model 2 with a different type of connection between steel elements

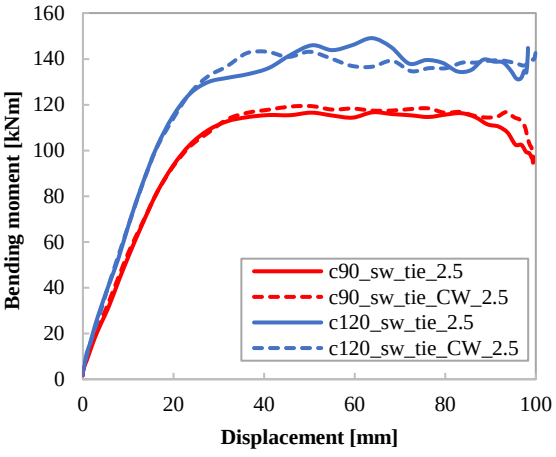

(d) models with a channel thickness of 2.5 mm and spot-welded steel elements

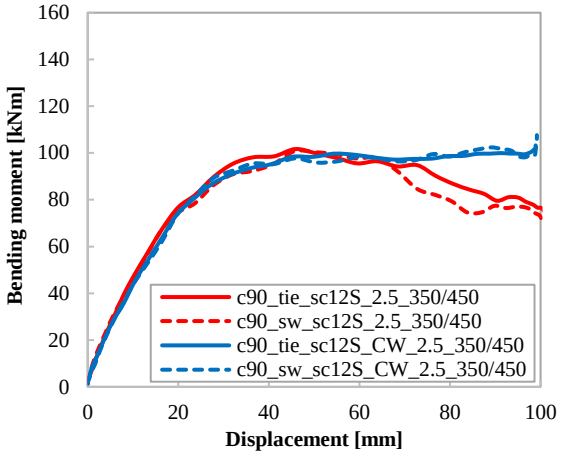

(e) models with a channel thickness of 2.5 mm and bolts 350/450

Figure 21. Influence of spot weld density

4.2.5. Corrugated Web in the Composite Beam

The CW with a thickness of 1.0 mm inserted between channels aims to increase the steel beam global stability resistance. In a composite solution, such stability issues are prevented with a concrete slab, but the increased distance between the channels consequently increases the distance between shear connectors. Consequently, the beam bending capacity is increased. Because of an increased distance between the shear connectors, the crushing of concrete is prevented in the area of one shear connector from extending to the area of the action of the other shear connector, which is placed in the same rib. The comparison of results for models with and without CW are shown in Figures 22-a to 22-d.

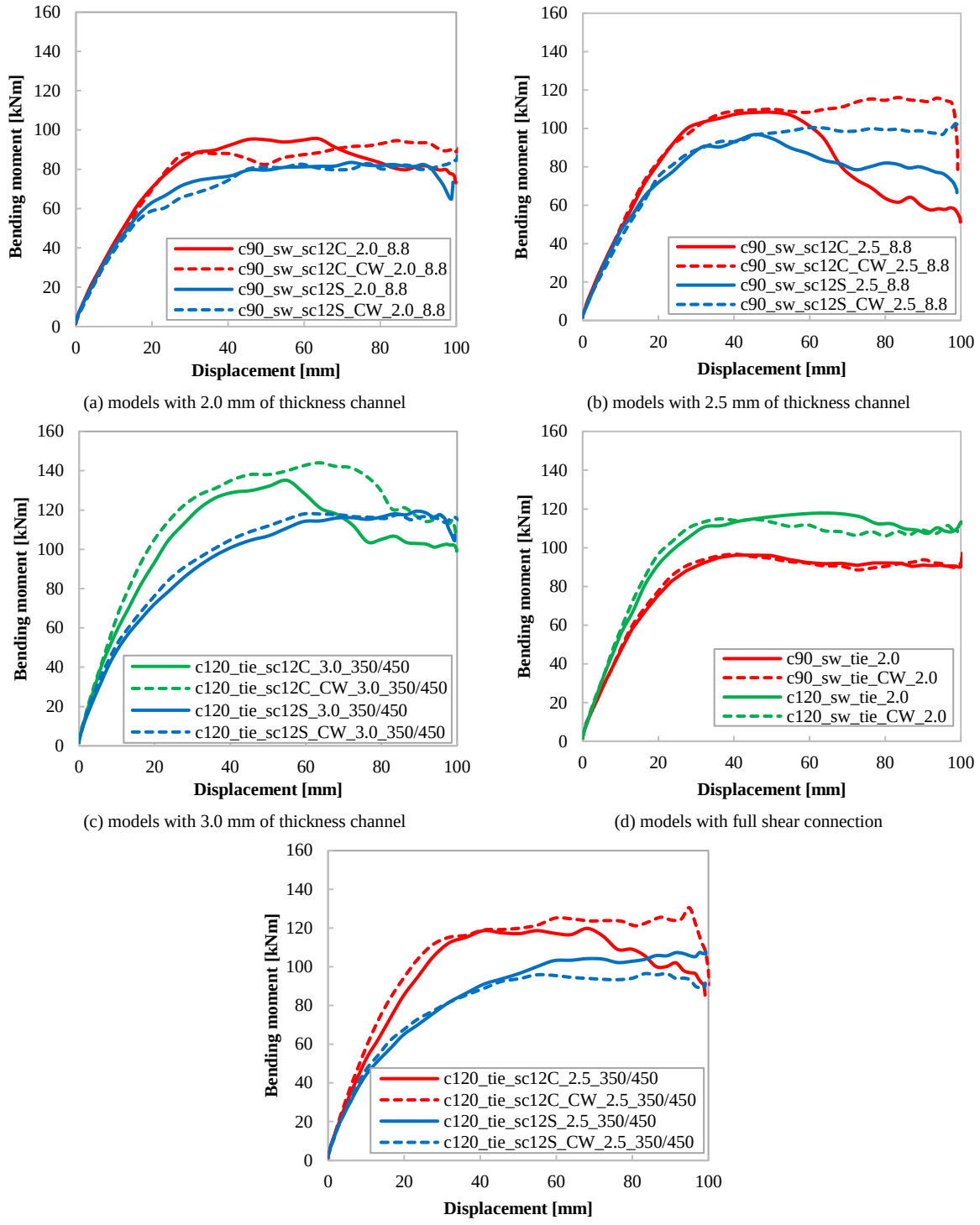

(a) models with 2.0 mm of thickness channel

(b) models with 2.5 mm of thickness channel

(c) models with 3.0 mm of thickness channel

(d) models with full shear connection

(e) models with tied steel elements

Figure 22. Influence of CW in composite beam

Results confirm the influence of increased distance between shear connectors. Models with CW and 2.5 mm and 3.0 mm channel thicknesses have achieved higher bending capacities and flexural stiffness than those without the CW. In addition, the results show that the models with CW can provide better ductility.

4.2.6. Concrete Slab Height

Figures 23-a to 23-d show the influence of the concrete slab configuration. As mentioned before, two different configurations of the concrete slab were investigated: a solid slab with a height of 90 mm (c90) and a concrete slab performed on a profiled metal sheet with an overall height of 120 mm (c120).

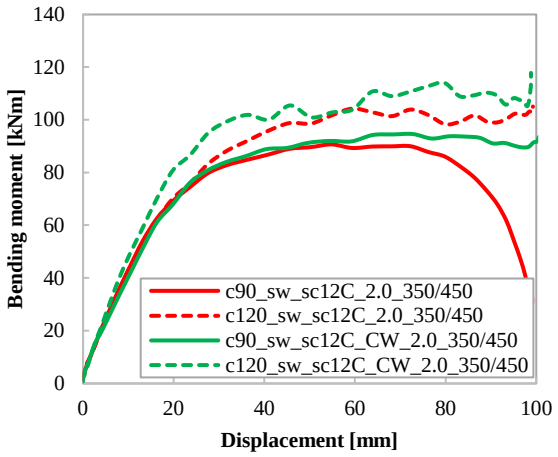

(a) models with 2.0 mm of thickness channel

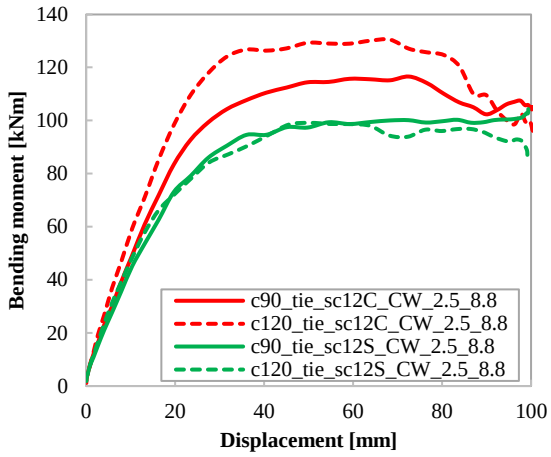

(b) models with 2.5 mm of thickness channel and bolts quality of 8.8

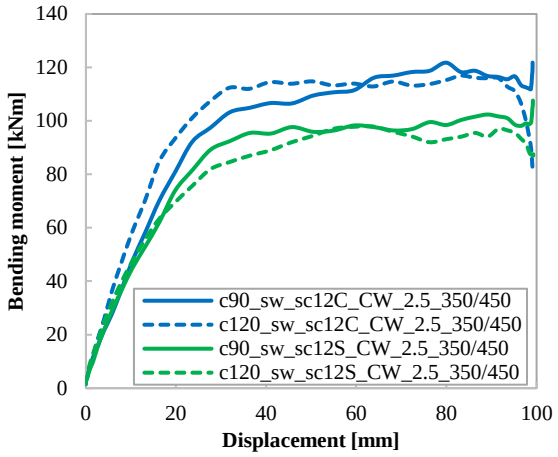

(c) models with 2.5 mm of thickness channel and bolts quality of 350/450

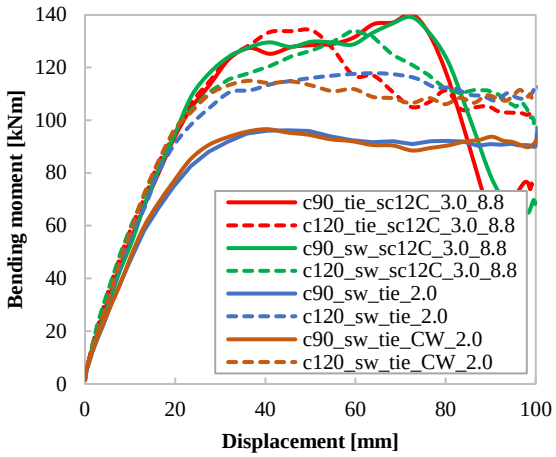

(d) models with 3.0 mm of thickness channel and bolts quality of 8.8

Figure 23. The influence of the concrete slab configuration

Figure 23-a shows the influence of the concrete slab height for models with and without CW. In Figures 23-b and 23-c, the influence of the concrete slab height is shown for models with different degrees of shear connection. An increase in bending capacity is observed for continuous shear connection and tie connection between steel elements, while the influence is negligible for other cases. Figure 23 (d) shows the influence of the concrete slab height for models with different channel thicknesses and different degrees of shear connection with and without CW. It can be observed that full shear connection increases beam bending capacity and flexural stiffness, depending on concrete slab configuration, while other parameters have negligible influence. From all presented results, it is concluded that the concrete slab configuration has a small influence on the beam bending capacity. At the same time, a certain increase in flexural stiffness can be observed for models with concrete slabs performed on a profiled metal sheet with an overall height of 120 mm (c120).

4.3. Comparison of Analytical and Numerical Results

Figures 24-a to 24-c show the comparison between analytically calculated characteristic bending resistances and the numerically obtained bending capacities for models with solid slab and tied steel elements (tie) and models with spot welded (sw) steel elements. Considering that in analytical approaches, it is not possible to consider the number and position of spot welds and the CW between channels, those influences are not considered. Figure 25-a to 25-c shows that numerically obtained bending capacities for full shear connection (tie) and the case when shear connectors are arranged in pairs (sc12C) reached all three analytically calculated values. In contrast, analytically calculated values are not reached when shear connectors are in a staggered arrangement (sc12S).

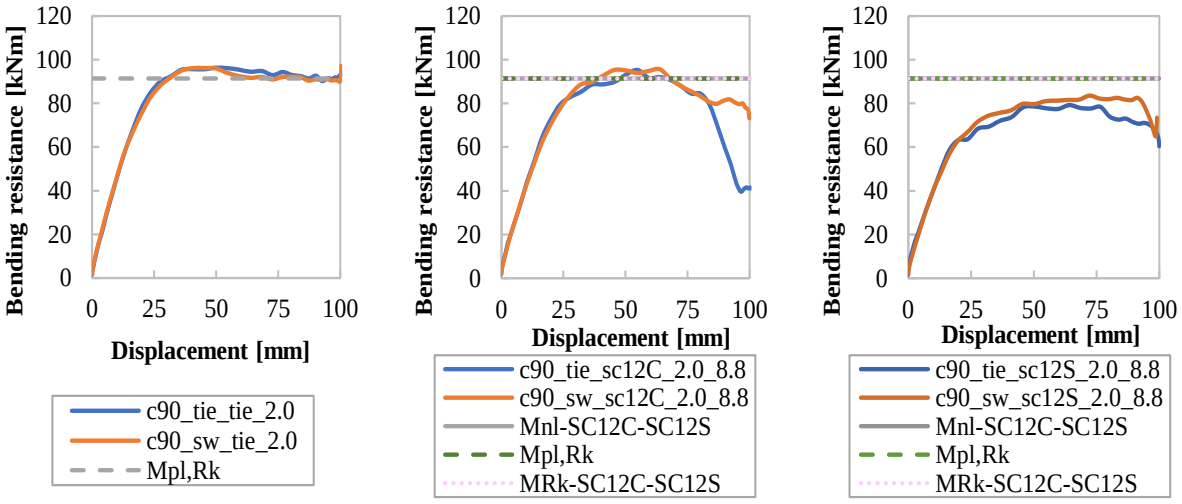

(a) full shear connection (b) bolts arranged in pairs (c) bolts in a staggered arrangement

Figure 24. Comparison of numerical and analytical models for channel thickness of 2.0 mm

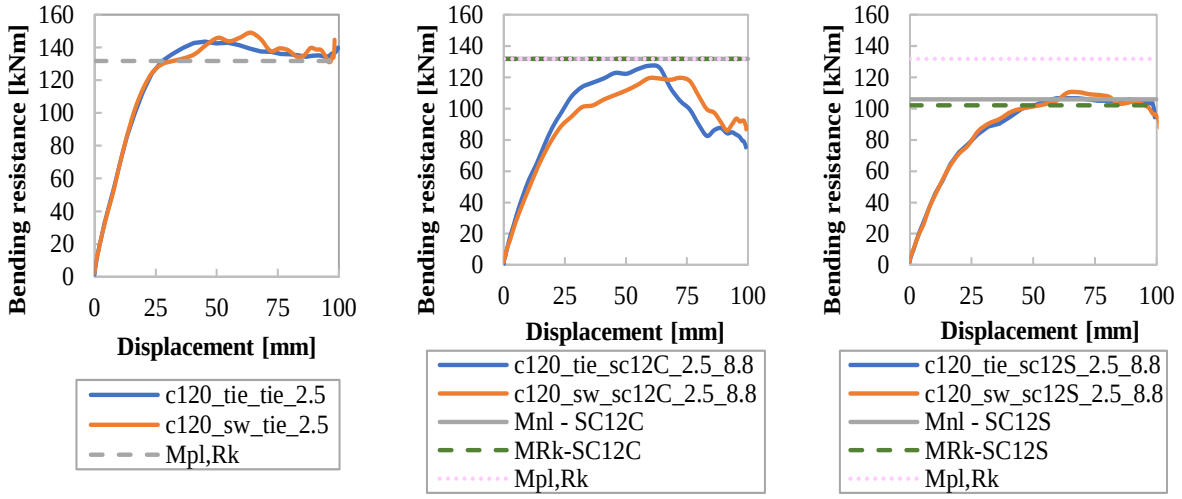

(a) full shear connection (b) bolts arranged in pairs (c) bolts in a staggered arrangement

Figure 25. Comparison of numerical and analytical models for channel thickness of 2.5 mm

Analysing Figure 24-b, where the results of numerical (models without CW and with concrete slab on a metal sheet) and analytical cases (for channel thickness of 2.5 mm) are shown. The results are achieved for all three analytical approaches. Figure 24-c shows the results in the case of full shear connection for the beam without CW and with a solid slab where the channel thickness is 3.0 mm and where the values of analytical resistances for plastic bending resistance and non-linear bending resistances (propped system) are achieved.

The values of the calculated plastic bending resistance for the full shear connection (according to Equation 2) and those calculated by modification of the equation for the partial shear connection, Equation 11, are shown in Tables 1 to 4. Figures 24-a to 24-c show the comparison of results given by analytical approaches (Tables 1 to 4) and numerical results.

From Figures 25-a to 25-c, which show results for models with metal sheets, it is possible to see that for the cases of full shear connection (or in the case when the arrangement of bolts results in the full shear connection), the values for non-linear bending resistance (propped system) and plastic bending resistance are the same. The values mentioned are different in the case of a partial shear connection.

Figure 26 compares numerical and analytical results for both concrete heights and full shear connection. From Figure 26, it is possible to see that numerical models achieved analytical results. However, from all presented comparisons, it can be concluded that there is a necessity to refine the analytical procedure to remain within the elastic limit considering all flexibility in the model.

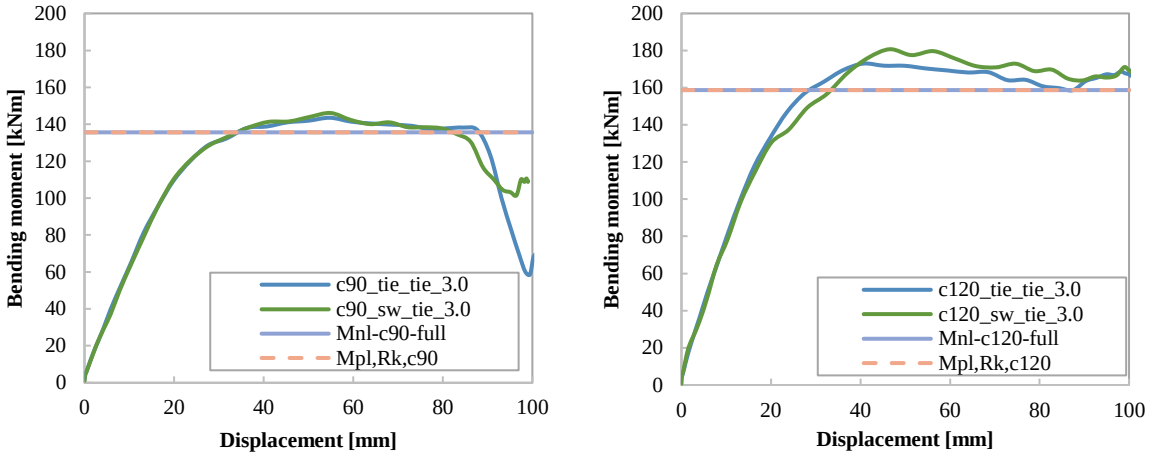

a) concrete slab height of 90 mm

b) concrete slab height of 120 mm

Figure 26. Comparison of numerical and analytical models for channel thickness of 3.0 mm

5. Conclusions

This research compares analytically obtained results from three approaches and numerical parametric results. Two configurations of concrete slabs were analysed: solid or slab on a profiled metal sheet. Furthermore, the study investigates the influence of the connection between steel elements as well as the presence of CW between back-to-back channels and channel thickness. Also, the research considers the influence of the degree of shear connection on the bending capacity but also the quality of shear connectors. The following conclusions are obtained:

- The obtained results showed that the bending capacity increased in models with slabs on the profiled metal sheet. It is expected because of the larger distance between the concrete part of the beam and the steel section.
- Discrete connections between steel elements have a negligible impact on the behaviour of steel back-to-back cross-sections in the analysed composite system.
- Results of models with CW between channels show that an extra element between channels does not increase the bending capacity of the composite section in the case of a continuous slab. A certain difference is observed in the case of a concrete slab on a profiled metal sheet. In addition, due to the larger distance between the shear connectors, the CW beam in the case of shear connectors in pairs shows increased bending capacity compared to models without CW.
- Observing the influence of the degree of shear connection shows that the degree of shear connection significantly affects bending capacity.
- A high influence on the bending capacity is noticeable by changing the thickness of the steel section.
- Good concordance of results is observed between the numerical model with a full shear connection and the analytical results for the full shear connection calculated according to the expression for the plastic bending resistance.
- The comparison of the numerical and analytical results shows that the bending resistances calculated according to the modified EN 1994-1-1 model for partial shear connections are in good agreement.
- Comparing the non-linear bending resistance and numerical results, it is visible that numerical models achieve all values calculated by the non-linear analytical approach.
- The results show that, compared to hot-rolled steel sections, the analysed, built-up CFS-concrete composite beams can provide excellent bending resistance.

This research provides information on several influences that could affect the bending resistance of the analysed built-up steel-concrete composite beam and an overview of three possible analytical approaches for its bending resistance calculation. Considering that the modified EN 1994-1-1 approach for partial shear connection gives results that are in good agreement with numerically obtained results, it can be assumed that this calculation method gives results close to the real ones. However, further laboratory and numerical investigations will provide more insight into the overall behaviour of the analysed system. Laboratory research will provide more knowledge about used materials (concrete, metal sheets, and shear connectors), spot welds, and support conditions. This will result in calibrated numerical models for further parametric studies. Also, future research will investigate a more accurate analytical approach to the bending resistance of such or similar floor systems. Considering that there is no proposed analytical equation for the bending resistance of a back-to-back built-up cold-formed steel-concrete beam, this should inspire researchers with the same or similar cross-section of the composite beam to investigate and publish their knowledge and findings.

6. Declarations

6.1. Author Contributions

Conceptualisation, A.R. and I.L.; methodology, A.R. and I.L.; software, A.R. and I.L; validation, I.L., D.S. and V.U.; formal analysis, A.R.; investigation, A.R. and I.L.; resources, A.R. and I.L., data curation, A.R.; writing—original draft preparation, A.R. and I.L.; writing—review and editing, A.R., I.L., D.S. and V.U.; visualisation, A.R.; supervision, I.L., D.S., and V.U.; project administration, A.R. and I.L.; funding acquisition, I.L. All authors have read and agreed to the published version of the manuscript.

6.2. Data Availability Statement

The data presented in this study are available in the article.

6.3. Funding

This research was partially funded by the Croatian Science Foundation, grant number UIP-2020-02-2964 (LWT-FLOOR project—Innovative lightweight cold-formed steel–concrete composite floor system), project leader: Ivan Lukačević.

6.4. Conflicts of Interest

The authors declare no conflict of interest.

7. References

[1] Lukačević, I., Ungureanu, V., Valčić, A., & Ćurković, I. (2021). Numerical study on bending resistance of cold-formed steel back-to-back built-up elements. Ce/Papers, 4(2–4), 487–494. doi:10.1002/cepa.1320.

[2] Selvaraj, S., & Madhavan, M. (2021). Design of Cold-Formed Steel Back-To-Back Connected Built-up Beams. Journal of Constructional Steel Research, 181, 106623. doi:10.1016/j.jcsr.2021.106623.

[3] Chen, B., Roy, K., Fang, Z., Uzzaman, A., Raftery, G., & Lim, J. B. P. (2021). Moment capacity of back-to-back cold-formed steel channels with edge-stiffened holes, un-stiffened holes, and plain webs. Engineering Structures, 235, 112042. doi:10.1016/j.engstruct.2021.112042.

[4] Ungureanu, V., Both, I., Burca, M., Grosan, M., Neagu, C., & Dubina, D. (2018). Experimental investigations on built-up cold-formed steel beams connected by resistance spot welding. Proceedings 12th International Conference on Advances in Steel-Concrete Composite Structures - ASCCS 2018. doi:10.4995/asccs2018.2018.7169.

[5] Both, I., Ungureanu, V., Tunea, D., Crisan, A., & Grosan, M. (2018). Experimental and numerical investigations on cold- formed steel beams assembled by MIG brazing. International Conference on Engineering Research and Practice for Steel Construction (ICSC2018), 5-7 September 2018, Hong Kong.

[6] Ungureanu, V., Both, I., Burca, M., Radu, B., Neagu, C., & Dubina, D. (2021). Experimental and numerical investigations on built-up cold-formed steel beams using resistance spot welding. Thin-Walled Structures, 161, 107456. doi:10.1016/j.tws.2021.107456.

[7] Ungureanu, V., Both, I., Tunea, D., Grosan, M., Neagu, C., Georgescu, M., & Dubina, D. (2018). Experimental investigations on built-up cold-formed steel beams using MIG brazing. Proceedings of the Eighth International Conference on Thin-Walled Structures-ICTWS, 24-27 July, 2018, Lisbon, Portugal.

[8] Kouider, N., Hadidane, Y., & Benzerara, M. (2021). Numerical investigation of the cold-formed I-beams bending strength with different web shapes. Frattura ed Integrita Strutturale, 16(59), 153–171. doi:10.3221/IGF-ESIS.59.12.

[9] Alharthi, Y. M., Sharaky, I. A., & Elamary, A. S. (2021). Numerical Analysis of Hybrid Steel Beams with Trapezoidal Corrugated Web Nonwelded Inclined Folds. Advances in Civil Engineering, 2021. doi:10.1155/2021/9918967.

[10] Górecki, M., & Śledziewski, K. (2022). Influence of corrugated web geometry on mechanical properties of I-beam: Laboratory tests. Materials, 15(1), 277. doi:10.3390/ma15010277.

[11] Mohamed, A., Tohamy, S., Saddek, A., & Drar, A. (2022). Numerical Investigation of Flange Buckling Behavior of Steel Plate Girders with Corrugated Webs. Sohag Engineering Journal, 2(1), 41–47. doi:10.21608/sej.2022.120610.1009.

[12] Hasan, Z. K., Hemzah, S. A., & Al-Kannoon, M. A. A. K. (2021). Behavior of corrugated steel compact I-section beams. Journal of Physics: Conference Series, 1895(1). doi:10.1088/1742-6596/1895/1/012063.

[13] Fang, Z., Roy, K., Liang, H., Poologanathan, K., Ghosh, K., Mohamed, A. M., & Lim, J. B. P. (2021). Numerical simulation and design recommendations for web crippling strength of cold-formed steel channels with web holes under interior-one-flange loading at elevated temperatures. Buildings, 11(12), 666. doi:10.3390/buildings11120666.

[14] Hsu, C. T. T., Punurai, S., Punurai, W., & Majdi, Y. (2014). New composite beams having cold-formed steel joists and concrete slab. Engineering Structures, 71, 187–200. doi:10.1016/j.engstruct.2014.04.011.

[15] Bamaga, S. O., Tahir, M. M., Ngian, S. P., Mohamad, S., Sulaiman, A., & Aghlara, R. (2019). Structural behaviour of cold-formed steel of double c-lipped channel sections integrated with concrete slabs as composite beams. Latin American Journal of Solids and Structures, 16(5), 1–15. doi:10.1590/1679-78255515.

[16] Elsawaf, S. A., & Bamaga, S. O. (2021). Strength capacity and failure mode of shear connectors suitable for composite cold formed steel beams: Numerical study. Materials, 14(13), 3627. doi:10.3390/ma14133627.

[17] Lukačević, I., Ćurković, I., Rajić, A., & Bartolac, M. (2022). Lightweight Composite Floor System—Cold-Formed Steel and Concrete—LWT-FLOOR Project. Buildings, 12(2), 209. doi:10.3390/buildings12020209.

[18] Nijgh, M. P., Gîrbacea, I. A., & Veljkovic, M. (2019). Elastic behaviour of a tapered steel-concrete composite beam optimized for reuse. Engineering Structures, 183, 366–374. doi:10.1016/j.engstruct.2019.01.022.

[19] Alhajri, T. M., Tahir, M. M., Azimi, M., Mirza, J., Lawan, M. M., Alenezi, K. K., & Ragaee, M. B. (2016). Behavior of pre-cast U-Shaped Composite Beam integrating cold-formed steel with ferro-cement slab. Thin-Walled Structures, 102, 18–29. doi:10.1016/j.tws.2016.01.014.

[20] Saggaff, A., Tahir, M. M., Azimi, M., & Alhajri, T. M. (2017). Structural aspects of cold-formed steel section designed as U-shape composite beam. AIP Conference Proceedings. doi:10.1063/1.5011505.

[21] Hosseini, S. M., Mashiri, F., & Mirza, O. (2021). Parametric study of innovative bolted shear connectors using 3D finite element modelling. Journal of Constructional Steel Research, 179, 106565. doi:10.1016/j.jcsr.2021.106565.

[22] Wang, W., Zhang, X. D., Zhou, X. L., Wu, L., & Zhu, H. J. (2021). Study on Shear Behavior of Multi-Bolt Connectors for Prefabricated Steel–Concrete Composite Beams. Frontiers in Materials, 8. doi:10.3389/fmats.2021.625425.

[23] Arévalo, D., Hernández, L., Gómez, C., Velasteguí, G., Guaminga, E., Baquero, R., & Dibujés, R. (2021). Structural performance of steel angle shear connectors with different orientation. Case Studies in Construction Materials, 14. doi:10.1016/j.cscm.2021.e00523.

[24] Lacki, P., Nawrot, J., Derlatka, A., & Winowiecka, J. (2019). Numerical and experimental tests of steel-concrete composite beam with the connector made of top-hat profile. Composite Structures, 211, 244–253. doi:10.1016/j.compstruct.2018.12.035.

[25] Jung, D. S., Park, S. H., Kim, T. H., Han, J. W., & Kim, C. Y. (2022). Demountable Bolted Shear Connector for Easy Deconstruction and Reconstruction of Concrete Slabs in Steel–Concrete Bridges. Applied Sciences (Switzerland), 12(3), 1508. doi:10.3390/app12031508.

[26] Talukder, M. M. H., Mouri, M. M., Singha, A., & Rahman, Md. S. (2021). Numerical Simulation of Steel Concrete Composite Floor System. Materials Science Forum, 1047, 195–201. doi:10.4028/www.scientific.net/msf.1047.195.

[27] Alwash, N. A., & Abd, N. H. (2021). Non-linear behavior of composite two way slab with screws as shear connectors under equivalent uniform distributed repeated load. Journal of Physics: Conference Series, 1973, 012036. doi:10.1088/1742-6596/1973/1/012036.

[28] Chung, W., & Sotelino, E. D. (2006). Three-dimensional finite element modeling of composite girder bridges. Engineering Structures, 28(1), 63–71. doi:10.1016/j.engstruct.2005.05.019.

[29] Bamaga, S. O., Tahir, M. M., Tan, C. S., Shek, P. N., & Aghlara, R. (2019). Push-out tests on three innovative shear connectors for composite cold-formed steel concrete beams. Construction and Building Materials, 223, 288–298. doi:10.1016/j.conbuildmat.2019.06.223.

[30] Wang, W., Zhang, X. dong, Zhou, X. long, Zhang, B., Chen, J., & Li, C. Hui. (2022). Experimental study on shear performance of an advanced bolted connection in steel-concrete composite beams. Case Studies in Construction Materials, 16. doi:10.1016/j.cscm.2022.e01037.

[31] Dai, X., Lam, D., Sheehan, T., Yang, J., & Zhou, K. (2018). Use of bolted shear connectors in composite construction. Proceedings 12th International Conference on Advances in Steel-Concrete Composite Structures - ASCCS 2018. doi:10.4995/asccs2018.2018.7039.

[32] Dias, J. V. F., Carvalho, H., Rodrigues, F. C., Maia, K. A. F. P., & Caldas, R. B. (2021). Experimental and numerical study on CFS composite beams with riveted shear connectors. Structures, 33, 737–747. doi:10.1016/j.istruc.2021.04.058.

[33] Vigneri, V., Odenbreit, C., & Romero, A. (2021). Numerical study on design rules for minimum degree of shear connection in propped steel–concrete composite beams. Engineering Structures, 241, 112466. doi:10.1016/j.engstruct.2021.112466.

[34] Classen, M. (2018). Limitations on the use of partial shear connection in composite beams with steel T-sections and uniformly spaced rib shear connectors. Journal of Constructional Steel Research, 142, 99–112. doi:10.1016/j.jcsr.2017.11.023.

[35] M.Irwan, J., Hanizah, A. H., & Azmi, I. (2009). Test of shear transfer enhancement in symmetric cold-formed steel-concrete composite beams. Journal of Constructional Steel Research, 65(12), 2087–2098. doi:10.1016/j.jcsr.2009.07.008.

[36] EN 1994-1-1. (2004). Eurocode 4: Design of composite steel and concrete structures - Part 1-1: General rules and rules for buildings. European Commitee for Standardization (CEN), Brussels, Belgium.

[37] Kyvelou, P., Gardner, L., & Nethercot, D. A. (2017). Design of Composite Cold-Formed Steel Flooring Systems. Structures, 12, 242–252. doi:10.1016/j.istruc.2017.09.006.

[38] Dujmović, D., Androić, B., & Lukačević, I. (2014). Composite Structures According to Eurocode 4. John Wiley & Sons, Hoboken, United States. doi:10.1002/9783433604908.

[39] ABAQUS. (2016). ABAQUS User's Manual. Dassault Systemes Simulia Corp, Rhode Island, United States.

[40] Ungureanu, V., Lukačević, I., Both, I., & Burca, M. (2019). Numerical investigation of built-up cold-formed steel beams connected by spot welding. Proceedings of the Evolving Metropolis, 2019 IABSE Congress, 4-6 September, 2019, New York, United States.

[41] EN 1992-1-1. (2011). Eurocode 2: Design of concrete structures - Part 1-1: General rules and rules for buildings. European Committee for Standardization (CEN), Brussels, Belgium.

[42] Pavlović, M., Marković, Z., Veljković, M., & Bucrossed D Signevac, D. (2013). Bolted shear connectors vs. headed studs behaviour in push-out tests. Journal of Constructional Steel Research, 88, 134–149. doi:10.1016/j.jcsr.2013.05.003.

[43] European standard EN 1993-1-1. (2005). Eurocode 3: Design of steel structures - Part 1-1: General rules and rules for buildings. European Committee for Standardization (CEN), Brussels, Belgium.